Inorganic Chemistry

pubs.acs.org/IC

Article

Synthesis and Chemistry of Ammonioethenyl and Phosphonioethenyl Ligands in Zwitterionic Dirhenium Carbonyl Complexes

Richard D. Adams,* Meenal Kaushal, Vitaly A. Rassolov, and Mark D. Smith

Cite This: *Inorg. Chem.* 2022, 61, 12262−12274

Read Online

ACCESS | Metrics & More | Article Recommendations | Supporting Information

ABSTRACT: New zwitterionic dirhenium carbonyl complexes containing ammonioethenyl and phosphonioethenyl ligands have been synthesized and studied. The reaction of $Re_2(CO)_{10}$ with C_2H_2 and Me_3NO yielded the dirhenium complex $Re_2(CO)_9(NMe_3)$ (**6**) and the new zwitterionic complex $Re_2(CO)_9[\eta^1\text{-}E\text{-}2\text{-}CH{=}CH(NMe_3)]$ (**7**). Compound **6** was characterized structurally and was found to have a NMe_3 ligand in an equatorial coordination site *cis* to a long Re−Re single bond, Re−Re = 3.0938(2) Å. Compound **7** can be obtained from the reaction of **6** with ethyne (C_2H_2) formally by the insertion of ethyne into the Re−N bond to the NMe_3 ligand. Compound **7** contains a 2-trimethylammonioethenyl ligand, $^-CH{=}CH(^+NMe_3)$, that is formally a zwitterion having a positive charge on the nitrogen atom and a negative charge on the terminal carbon atom. When coordinated to rhenium by the terminal ethenyl carbon atom, the negative charge on the $^-CH{=}CH(^+NMe_3)$ carbon atom is formally transferred to the rhenium atom. The reaction of $Re_2(CO)_{10}$ with C_2H_2 and NEt_3 in the presence of Me_3NO yielded the new dirhenium complex $Re_2(CO)_9[\eta^1\text{-}E\text{-}2\text{-}CH{=}CH(NEt_3)]$ (**8**) together with some **6** and **7**. Compound **8** is structurally similar to **7**, but it contains a NEt_3 group in the ammonioethenyl ligand in the place of the NMe_3 group in **7**. Reactions of **7** with $PMePh_2$ and PPh_3 yielded the zwitterionic 2-arylphosphonioethenyl-coordinated dirhenium carbonyl complexes, $Re_2(CO)_9[\eta^1\text{-}E\text{-}2\text{-}CH{=}CH(PPh_2Me)]$ (**9a**) and $Re_2(CO)_9[\eta^1\text{-}E\text{-}2\text{-}CH{=}CH(PPh_3)]$ (**9b**), and the zwitterionic 1-phosphonioethenyl ligand in the dirhenium carbonyl complexes, $Re_2(CO)_9[\eta^1\text{-}1\text{-}C(PPh_2Me)(=CH_2)]$ (**10a**), $Re_2(CO)_8[\mu\text{-}\eta^2\text{-}1\text{-}C(PPh_2Me)(=CH_2)]$ (**11a**), and $Re_2(CO)_8[[\mu\text{-}\eta^2\text{-}1\text{-}C(PPh_3)(CH_2)]$ (**11b**). Compound **10a** was converted to **11a** and the new compound $Re_2(CO)_7(\mu\text{-}H)[\mu\text{-}\eta^2\text{-}1\text{-}(CH_2C)P(Ph)(Me)(o\text{-}C_6H_4)]$, (**12**) by decarbonylation using Me_3NO. Compound **12** contains an *ortho*-metalated phenyl ring. The new products **6**,**7**, **8**, **9b**, **10a**, **11a**, **11b** and **12** were characterized structurally by single-crystal X-ray diffraction analyses.

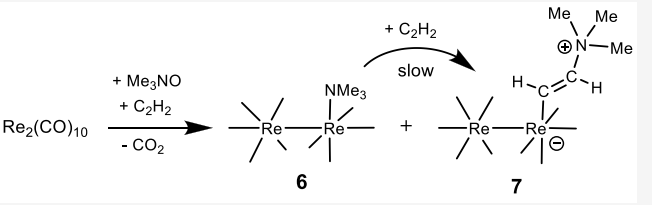

INTRODUCTION

Hydrocarbyl zwitterions containing phosphorus and sulfur substituents, such as the phosphorus and sulfur ylides, **A**[1] and **B**,[2] Scheme 1, are valuable reagents in organic synthesis.[2−4]

Scheme 1. Sketches of Some of the Classical Onium Hydrocarbyl Zwitterions

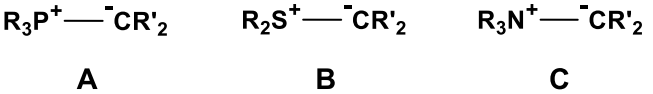

Ammonium ylides **C** are less stable then their phosphonium and sulfonium cousins, but recent studies have shown that they can be important intermediates in organic transformations.[5]

These ylides can serve as good ligands and are stabilized by the coordination of the negatively charged carbon atom to metal atoms **M**, e.g., **D** and **E**. The metal complexes are also zwitterions that are formed by a formal transfer of the negative charge on the ylide carbon atom to the metal atom (Scheme 2).[6,7]

Scheme 2. Sketches of Some of the Classical Onium Hydrocarbyl Zwitterions Serving as Ligands

In recent years, families of metal-stabilized, unsaturated zwitterionic hydrocarbyl ligands have begun to appear. Some representative examples are shown in the structures **F**−**I** (Scheme 3).[8−12] They can be obtained by the addition of tertiary phosphines to certain alkyne or vinylidene ligands.

Received: April 28, 2022
Published: July 27, 2022

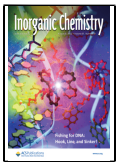

https://doi.org/10.1021/acs.inorgchem.2c01471
Inorg. Chem. 2022, 61, 12262−12274

Scheme 3. Sketches of Some Metal Complexed Unsaturated Onium Hydrocarbyl Zwitterions Serving as Ligands

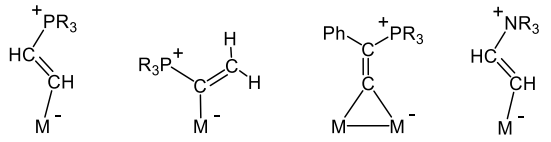

These ligands have the potential for new organic transformations and organic synthesis. There are very few examples of complexes containing the ammonioethenyl ligands as represented by the structure **I**.[13−15]

The first example of an ammonioethenyl ligand was obtained by Chin et al. for the iridium complex ion $[Ir(H)(C_2Ph)(-CH{=}CH-NEt_3)(CO)(PPh_3)_2]^+$ in 1997 from the reaction of the salt $[Ir(H)(C_2Ph)(NCPh)(CO)(PPh_3)_2][ClO_4]$ with a mixture of ethyne and NEt_3.[13] In recent studies, we have synthesized a number of new examples including the first examples of bridging η^2-trimethylammonioethenyl ligands in the zwitterionic polynuclear ruthenium carbonyl complexes $Ru_6(\mu_6\text{-}C)(CO)_{15}(\mu\text{-}\eta^2\text{-}CHCHNMe_3)$ (**1**)[14] and $Ru_5(\mu_6\text{-}C)(CO)_{13}(\mu\text{-}\eta^2\text{-}CHCHNMe_3)$ (**2**).[15] These bridging η^2-ligands were readily converted to terminally coordinated η^1-ligands as found in the complexes $Ru_6(\mu_6\text{-}C)(CO)_{16}[\mu\text{-}\eta^1\text{-}E\text{-}CH{=}CH(NMe_3)]$ (**3**)[14] and $Ru_5(\mu_5\text{-}C)(CO)_{14}[\mu\text{-}\eta^1\text{-}E\text{-}CH{=}CHNMe_3)$ (**4**)[15] by the addition of CO to **1** and **2**, respectively (eqs 1 and 2 in Scheme 4).

Scheme 4. Schematics of Two Reactions Showing the Transformations of Bridging Ammonioethenyl Ligands into Terminal Ammonioethenyl Ligands by the Addition of CO to Ruthenium Cluster Complexes[14,15a]

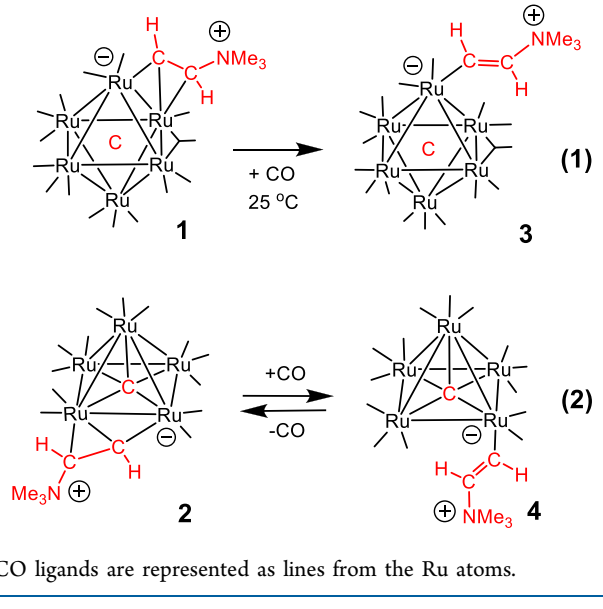

[a]CO ligands are represented as lines from the Ru atoms.

Interestingly, it was found that ethyne (C_2H_2) can be added to the bridging η^2-CHCH($^+NMe_3$) ligand in **1** to form a triply bridging η^4-trimethylammoniobutadienyl, $(\mu_3\text{-}\eta^4\text{-}CHCHCH^+NMe_3)$, ligand in the zwitterionic complex $Ru_6(\mu_6\text{-}C)(CO)_{14}[\mu_3\text{-}\eta^4\text{-}C_4H_4(NMe_3)]$ (**5**) by the formation of a C−C bond to the bridging η^2-CHCH($^+NMe_3$) ligand in **1** (Scheme 5).

Scheme 5. Schematic Showing the Addition and Coupling of Ethyne to the β-Carbon Atom of the Bridging Ammonioethenyl Ligand in 1[a]

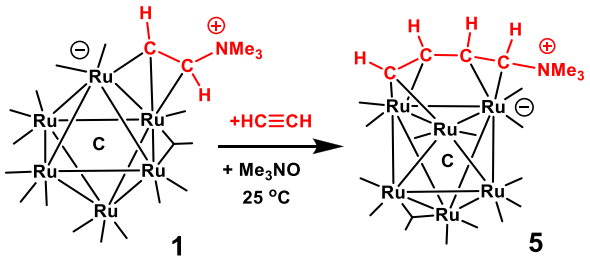

[a]CO ligands are represented as lines from the Ru atoms.[14]

Our most recent studies have been focused on reactions of the dirhenium carbonyl complex $Re_2(CO)_{10}$ with ethyne and combinations of NMe_3 or NEt_3 in the presence of Me_3NO. New dirhenium carbonyl complexes containing terminally coordinated, ammonioethenyl, η^1-*E*-CH=CH($^+NR_3$) (R = Me, Et) ligands have been obtained. It has also been found that the tertiary amino group can be replaced in reactions with the tertiary phosphines PPh_3 and $PMePh_2$ to yield dirhenium complexes containing the phosphonioethenyl ligands: η^1-2-CH=CH($^+PR_3$), η^1-1-C($^+PR_3$)=CH_2, and μ-η^2-1-C($^+PR_3$)=CH_2 (R_3 = Ph_3 and $MePh_2$). The syntheses, structures, and chemistry of these new dirhenium complexes are described in this report.

EXPERIMENTAL SECTION

General Data. All reactions were performed under a nitrogen atmosphere. Reagent-grade solvents were dried by the standard procedures and were freshly distilled prior to use. Infrared spectra were recorded on a Nicolet IS10 midinfrared FT-IR spectrophotometer. ^1H NMR spectra were recorded on a Bruker AVANCE III-HD 300 spectrometer operating at 300.1 MHz. ^{31}P NMR spectra were recorded on a Bruker AVANCE III-HD 300 operating at 121.5 MHz. ^{13}C NMR spectra were recorded on a Bruker AVANCE III-HD 400 spectrometer operating at 100.65 MHz. Mass spectrometric (MS) measurements performed by a direct-exposure probe by using electron impact ionization (EI) were made on a VG 70S instrument. $Re_2(CO)_{10}$, trimethylamine oxide, acetylene (industrial-grade C_2H_2), triphenylphosphine, and methyldiphenylphosphine were obtained from Pressure Chemicals, Tokyo Chemical Industry, Praxair, Columbia Organic Chemicals Company, and Sigma-Aldrich Chemical Co., respectively. All reagents were used as received. Product separations were performed by TLC in air on Analtech 0.25 or 0.50 mm silica gel 60 Å F_{254} glass plates.

WARNING! *Carbon monoxide and ethyne are hazardous gases that should be used only in a well-ventilated fume hood.*

*Reaction of $Re_2(CO)_{10}$ with C_2H_2 in the Presence of Me_3NO: Syntheses of $Re_2(CO)_9(NMe_3)$ (**6**) and $Re_2(CO)_9[\eta^1\text{-}E\text{-}2\text{-}CH{=}CH(NMe_3)]$ (**7**).* A 50.0 mg (0.0766 mmol) amount of $Re_2(CO)_{10}$ was dissolved in 1.5 mL of CD_2Cl_2 in a 5 mm NMR tube. The tube was evacuated and filled with acetylene. A 17.0 mg (0.227 mmol) portion of Me_3NO was dissolved in CD_2Cl_2 and then added to the NMR tube. The color of the solution changed from colorless to yellow upon addition. The NMR tube was allowed to stand for 15 min. The solvent was removed in vacuo. The residue was extracted in CH_2Cl_2 and separated by TLC by using a 3:1 hexane/CH_2Cl_2 (v/v) solvent mixture to yield two products in order of elution: a bright-yellow band of $Re_2(CO)_9(NMe_3)$ (**6**),[16] 8.0 mg (15% yield), and a pale-yellow band of $Re_2(CO)_9[\eta^1\text{-}E\text{-}2\text{-}CH{=}CH(NMe_3)]$ (**7**), 13.0 mg (25% yield). Compound **6** is unstable in solution in the open air and undergoes significant decomposition in 10−30 min. Crystalline forms of **6** are more stable. Compound **7** is much more stable than **6** in the

https://doi.org/10.1021/acs.inorgchem.2c01471
Inorg. Chem. 2022, 61, 12262−12274

open air both in the solid state and in solution. Spectral data for **6**: IR ν_{CO} (cm^{-1} in CH_2Cl_2): 2102 (w), 2034 (s), 1986 (vs) 1952 (m) 1911 (m). ^1H NMR (CD_2Cl_2, δ in ppm) 3.05 (s, 9H). Mass spectra (EI/MS m/z): 683, M^+, 624 $M^+ - NMe_3$. The isotope distribution pattern is consistent with the presence of two rhenium atoms. Spectral data for **7**: IR ν_{CO} (cm^{-1} in CH_2Cl_2): 2089 (m), 2025 (s), 1973 (vs), 1936 (s), 1894 (s). ^1H NMR (CD_2Cl_2, δ in ppm): 7.80 (d, 1H, CH, $^3J_{H-H}$ = 15 Hz), 5.62 (d, 1H, CH, $^3J_{H-H}$ = 15 Hz), 3.01 (s, 9H, NMe_3). ^{13}C NMR (CD_2Cl_2, 125.79 MHz, δ in ppm): 200.92 (CO), 199.38 (CO), 195.05 (CO), 191.66 (CO), 134.41 (=CH), 128.34 (=CH), and 54.49 (3 CH_3). Elemental analysis: Calculated for $Re_2NO_9C_{14}H_{11}$: C, 23.69%; H, 1.56%; N, 1.97%. Found: C, 23.68%; H, 1.68%; N, 1.99%.

*Direct Synthesis of $Re_2(CO)_9(NMe_3)$ (**6**).* A 50.0 mg (0.0766 mmol) portion of $Re_2(CO)_{10}$ was dissolved in 1.5 mL of CD_2Cl_2 in a 5 mm NMR tube. A 17.0 mg (0.227 mmol) amount of Me_3NO was dissolved in CD_2Cl_2 and then added to the NMR tube. The color changed from colorless to yellow upon addition. The NMR tube was allowed to stand for 15 min. The solvent was removed *in vacuo*. The residue was extracted in CH_2Cl_2 and separated with TLC by using hexane solvent to give a bright-yellow band of $Re_2(CO)_9(NMe_3)$ (**6**), 21.0 mg (40% yield). The first evidence of the existence of **6** was obtained by Bergamo et al. in their studies of the reactions of $Re_2(CO)_{10}$ with Me_3NO in tetrahydrofuran solvent, but it was not isolated.[16]

*Synthesis of $Re_2(CO)_9[\eta^1$-E-2-CH=CH(NMe$_3$)] (**7**) from **6** and C_2H_2.* An 8.0 mg (0.0117 mmol) amount of **6** was dissolved in 1.5 mL of CD_2Cl_2 in a 5 mm NMR tube. The tube was evacuated and filled with acetylene gas and was then allowed to stand for 24 h at room temperature. The product was isolated by TLC by using a 3:1 hexane/CH_2Cl_2 (v/v) solvent mixture to yield 4.0 mg of $Re_2(CO)_9[\eta^1$-*E*-2-CH=CH(NMe_3)] (**7**) (48% yield).

*Synthesis of $Re_2(CO)_9[\eta^1$-E-2-CH=CH(NEt$_3$)] (**8**) from $Re_2(CO)_{10}$ with C_2H_2 and NEt$_3$ in the Presence of Me_3NO.* A 30.0 mg (0.0460 mmol) amount of $Re_2(CO)_{10}$ was dissolved in 1.5 mL of CD_2Cl_2 in a 5 mm NMR tube. A 13 μL (0.0920 mmol) portion of NEt_3 was then added to the NMR tube. The tube was shaken and then evacuated and filled with acetylene. A 10.0 mg (0.138 mmol) amount of Me_3NO was dissolved in CD_2Cl_2 and then added to the NMR tube. The color changed from colorless to yellow upon addition. The products were isolated by TLC by using a 2:1 hexane/CH_2Cl_2 (v/v) solvent mixture to yield two products in order of elution: a bright-yellow band of **6**, 2.0 mg (6% yield), and two pale-yellow bands consisting of $Re_2(CO)_9[\eta^1$-*E*-2-CH=CH(NEt_3)] (**8**), 7.0 mg (20% yield), followed by **7**, 6.0 mg (18% yield). Spectral data for **8**: IR ν_{CO} (cm^{-1} in CH_2Cl_2): 2088 (w), 2023 (m), 1973 (s), 1935 (m), 1893 (m). ^1H NMR (CD_2Cl_2, δ in ppm): 7.62 (d, 1H, CH, $^3J_{H-H}$ = 16.2 Hz), 5.20 (d, 1H, CH, $^3J_{H-H}$ = 16.2 Hz), 3.10 (q, 6H, NCH_2CH_3, ^3J = 7.2 Hz), 1.24 (t, 9H, NCH_2CH_3, ^3J = 7.2 Hz). Mass spectra (EI/MS m/z): 751, M^+; 723 $M^+ - CO$. The isotope distribution pattern is consistent with the presence of two rhenium atoms.

*Reaction of **7** with $PMePh_2$.* A 50.0 mg (0.0705 mmol) amount of **7** and 30 μL (0.1612 mmol) of $PMePh_2$ were dissolved in 1.5 mL of CD_2Cl_2 in a 5 mm NMR tube. The NMR tube was evacuated and filled with nitrogen and was then held at 45 °C for 24 h. A ^1H NMR spectrum obtained after this period showed new resonances at δ = 2.41−2.50, 4.15−4.20, 6.53−6.74, 6.75−7.22, and 10.02−10.22. The solution was then cooled to room temperature, and the solvent was removed *in vacuo*. The products were isolated by TLC by using a 4:1 hexane/CH_2Cl_2 (v/v) solvent mixture to give the following in order of elution: two yellow bands of $Re_2(CO)_8[\mu$-η^2-C(=CH_2)-(PPh_2Me)], **11a**, 5.0 mg (9% yield), and $Re_2(CO)_9[\eta^1$-C(=CH_2)(PPh_2Me)] (**10a**), 18.0 mg (30% yield), and a very pale yellow band of $Re_2(CO)_9[\eta^1$-*E*-2-CH=CH(PPh_2Me)] (**9a**), 19.0 mg (32% yield). Spectral data for **9a**: IR ν_{CO} (cm^{-1} in CH_2Cl_2): 2108 (w), 2089 (m), 2025 (s), 1977 (s), 1938 (m), 1900 (m). ^1H NMR (in CD_2Cl_2): δ 10.12 (dd, 1H, $^3J_{H-H}$ = 19.8 Hz, $^3J_{P-H}$ = 38.7 Hz, =C**H**P), 7.79−7.19 (m, 10H, 2Ph), 6.63 (dd, 1H, $^3J_{H-H}$ = 19.8 Hz, $^2J_{P-H}$ = 42.6 Hz, **H**C=CHP), 2.17 (d, 3H, $^2J_{P-H}$ = 12.6 Hz, PC**H**$_3$). ^{31}P NMR (CD_2Cl_2): δ 6.55. ^{13}C NMR (CD_2Cl_2, @100.65 MHz): δ 201.21 (2CO), 198.29 (br, 4CO), 197.45 (1CO, J_{CP} = 13 Hz), 196.05 (1CO, J_{CP} = 6 Hz), 191.99, (1CO), 133.83 (Ph, para **C**, J_{P-C} = 1.1 Hz), 132.26 (Ph, meta **C**, J_{P-C} = 9.8 Hz), 129.75 (Ph, ortho **C**, J_{P-C} = 12.1 Hz), 129.80 (Ph, ipso **C**, J_{P-C} = 217 Hz), 122.74 (HC**C**HP, $^1J_{P-C}$ = 85 Hz), 110.03 (H**C**CHP, $^2J_{P-C}$ = 66 Hz). Mass spectra (EI/MS m/z): 850, M^+; 822, $M^+ - CO$; 794, $M^+ - 2CO$. Spectral data for **10a**: IR ν_{CO} (cm^{-1} in CH_2Cl_2): 2092 (m), 2071 (w), 2022 (m), 1980 (s), 1949 (s), 1926 (w), 1984 (w). ^1H NMR (CD_2Cl_2, δ in ppm): 7.09 (dd, 1H, $^3J_{P-H}$ = 74.7 Hz, $^2J_{H-H}$ = 2.1 Hz); 7.63 (m, 9H), 6.82 (dd, 1H, $^3J_{P-H}$ = 43.2 Hz, $^2J_{H-H}$ = 2.1 Hz), 2.51 (d, 3H, $^2J_{P-H}$ = 12.6 Hz). ^{13}C NMR (CD_2Cl_2): δ 203.0 (CO), 198.2 (br, CO), 192.8 (CO), 154.0 (H_2CCP), 133.2 (Ph, para **C**, J_{P-C} = 2.8 Hz), 132.6 (Ph, meta **C**, J_{P-C} = 8.7 Hz), 129.5 (Ph, ortho **C**, J_{P-C} = 11.3 Hz), 129.0 (Ph, ipso **C**, J_{P-C} = 10.7 Hz), 123.7 (H_2CCP, $^1J_{P-C}$ = 76.9 Hz), 12.4 (P**C**H_3, $^1J_{P-C}$ = 63.8 Hz). ^{31}P NMR (CD_2Cl_2, δ in ppm): 32.90. Mass spectra (EI/MS m/z): 850, M^+; 794, $M^+ - 2CO$; 766, $M^+ - 3CO$. The isotope distribution pattern is consistent with the presence of two rhenium atoms. Spectral data for **11a**: IR ν_{CO} (cm^{-1} in CH_2Cl_2): 2088 (w), 2071 (m), 2024 (m), 1977 (m), 1952 (s), 1927 (s), 1908 (s). ^1H NMR (in CD_2Cl_2): δ 7.9−7.5 (m, 10H, 2Ph) 4.17 (dd, 1H, $^2J_{H-H}$ = 2.5 Hz, $^3J_{P-H}$ = 25 Hz, H**H**CCP), 2.46 (dd, 1H, $^2J_{H-H}$ = 2.5 Hz, $^3J_{P-H}$ = 42 Hz, **H**HCCP), 2.36 (d, 3H, $^2J_{P-H}$ = 11.5 Hz, P**Me**). ^{31}P NMR (CD_2Cl_2): δ 35.86. ^{13}C NMR (CD_2Cl_2, @100.65 MHz): δ 199.23 CO, 196.65 CO, 194.57 CO, 189.94 CO, 134.15 (Ph, para **C**), 134.06 (Ph2, para **C**), 133.27 (Ph1, meta **C**), 133.19 (Ph2, meta **C**), 133.18 (Ph1, ipso **C**, J_{P-C} = 58 Hz), 133.15 (Ph2, ipso **C**, J_{P-C} = 59 Hz), 129.03 (Ph1, ortho **C**, J_{P-C} = 11 Hz), 129.0 (Ph2, ortho **C**, J_{P-C} = 9 Hz), 104.71 (H_2CCP, $^2J_{P-C}$ = 9 Hz), 47.14 (H_2CCP), 9.18 (H_3CP, $^1J_{P-C}$ = 53 Hz). Mass spectra (EI/MS m/z): 822, M^+; 794, $M^+ - CO$; 766, $M^+ - 2CO$. The isotope distribution pattern is consistent with the presence of two rhenium atoms.

*Reaction of **7** with PPh_3.* A 25.0 mg (0.035 mmol) amount of **7** and a 24.0 mg (0.092 mmol) amount of PPh_3 were dissolved in 1.5 mL of CD_2Cl_2 in a 5 mm NMR tube. The NMR tube was evacuated and filled with nitrogen. The NMR tube was then held at 48 °C for 32 h. After cooling, the solvent was removed and the products were isolated by TLC by using 2:1 hexane/CH_2Cl_2 (v/v) to give the following in order of elution: a yellow band of $Re_2(CO)_8[\mu$-η^2−C(=CH_2)(PPh_3)] (**11b**), 10.0 mg (32% yield), and a pale-yellow band of $Re_2(CO)_9[\eta^1$-*E*-2-CH=CH(PPh_3)] (**9b**), 5.0 mg (16% yield). Spectral data for **9b**: IR ν_{CO} (cm^{-1} in CH_2Cl_2): 2090 (m), 2075 (w), 2025 (m), 1977 (s), 1937 (w), 1900 (w). ^1H NMR (in CD_2Cl_2): δ 10.10 (dd, 1H, $^3J_{H-H}$ = 19.5 Hz, $^3J_{P-H}$ = 36.9 Hz), 7.76−7.04 (m, 15H, 3Ph), 6.95 (dd, 1H, $^3J_{H-H}$ = 19.5 Hz, $^2J_{P-H}$ = 41.4 Hz). ^{31}P NMR (in CD_2Cl_2): δ 10.28. Mass spectra (EI/MS m/z): 884, M^+; 856, $M^+ - CO$; 828, $M^+ - 2CO$. The isotope distribution pattern is consistent with the presence of two rhenium atoms. Spectral data for **11b**: IR ν_{CO} (cm^{-1} in CH_2Cl_2): 2088 (w), 2070 (m), 2023 (s), 1976 (s), 1959 (m), 1946 (s), 1904 (m). ^1H NMR (CD_2Cl_2, δ in ppm): 7.78−7.46 (m, 15H, 3Ph), 4.36 (dd, $^2J_{H-H}$ = 2.1 Hz, $^3J_{P-H}$ = 25.2 Hz, CH**H**), 2.69 (dd, 1H, $^2J_{H-H}$ = 2.1 Hz, $^3J_{P-H}$ = 44.1 Hz, C**H**H). ^{31}P NMR (CD_2Cl_2, δ in ppm): 37.21. Mass spectra (EI/MS m/z): 856, $M^+ - CO$; 828, $M^+ - 2CO$; 800, $M^+ - 3CO$. The isotope distribution pattern is consistent with the presence of two rhenium atoms.

*Attempted Conversion of **9a** to **10a**/**11a**.* A 15.0 mg (0.0176 mmol) sample of **9a** was dissolved in 1.5 mL of toluene-d_8 in a 5 mm NMR tube and then held at 100 °C for 17 h. After this period, the NMR spectrum showed no evidence of the formation of **10a** or **11a**, and compound **9a** (13.0 mg) was recovered.

*Reaction of **10a** with Trimethylamine N-Oxide.* A 38.0 mg (0.045 mmol) amount of **10a** and a 5.0 mg (0.067 mmol) amount of Me_3NO were dissolved in 1.5 mL of CD_2Cl_2 in a 5 mm NMR tube. The NMR tube was evacuated and filled with nitrogen. The NMR tube was then heated to 48 °C for 2 h. A ^1H NMR spectrum obtained after this period showed a resonance at δ = −13.5 for a new compound and also the resonances of **11a**. The solution was then cooled to room temperature, and the solvent was removed *in vacuo*. The residue was extracted in CH_2Cl_2 and separated with TLC by using 1:1 hexane/CH_2Cl_2 (v/v) to give the following in order of elution: a colorless band of $Re_2(CO)_7(\mu$-H)[μ-η^2-(CH_2C)P(Ph)Me(*o*-C_6H_4)] (**12**), 3.0

https://doi.org/10.1021/acs.inorgchem.2c01471
Inorg. Chem. 2022, 61, 12262−12274

mg (8.5% yield), and a yellow band of **11a**, 20.0 mg (55% yield). Spectral data for **12**: IR ν_{CO} (cm^{-1} in hexane): 2088 (m), 2028 (s), 1988 (m), 1982 (s), 1955 (m), 1948 (s), 1931 (m). ^1H NMR (in CD_2Cl_2): δ 8.25−7.15 (m, 9H, Ph), 5.56 (d, 1H, $^3J_{P-H}$ = 30.6 Hz, CH**H**), 4.96 (d, 1H, $^3J_{P-H}$ = 42.6 Hz, C**H**H), 2.42 (d, 3H, $^2J_{P-H}$ = 12 Hz, P**Me**), −13.5 (s, 1H, Re**H**Re). ^{31}P NMR (CD_2Cl_2): δ 41.8. Mass spectra (EI/MS *m*/*z*): 794, M^+; 766, $M^+ - CO$; 738, $M^+ - 2CO$. The isotope distribution pattern is consistent with the presence of two rhenium atoms.

*Reaction of **11a** with CO.* A 10.0 mg (0.012 mmol) amount of compound **11a** was dissolved in 5 mL of C_6D_6 and transferred to a Parr high-pressure reaction vessel. The reaction vessel was then pressurized to 30 atm with CO gas and held at 80 °C for 40 h. A ^1H NMR spectrum obtained after this period showed that **11a** was converted to **10a**. The solution was then cooled and the solvent was removed *in vacuo*. The residue was extracted in CH_2Cl_2 and separated by TLC by using hexane to give 4.0 mg (39% yield) of **10a**. A 5.0 mg amount of unreacted **11a** was recovered.

Crystallographic Analyses. Yellow single crystals of **6** were obtained by the rapid evaporation of solvent from a solution in a mixture of hexane and dichloromethane at room temperature. Pale-yellow single crystals of **7** and **8**, yellow crystals of **9b**, and colorless single crystals of **12** suitable for X-ray diffraction analyses were obtained by the slow evaporation of solvent from a solution in a mixture of dichloromethane and hexane at 25 °C. Yellow single crystals of **10a**, **11a**, and **11b** suitable for X-ray diffraction analyses were obtained by the slow evaporation of solvent from a solution in a mixture of benzene and hexane at 25 °C. All of the crystal data were collected at 100(2) K by using a Bruker D8 QUEST diffractometer equipped with a PHOTON-100 CMOS area detector and an Incoatec microfocus source (Mo Kα radiation, λ = 0.71073 Å).[17] The raw area detector data frames were reduced, scaled, and corrected for absorption effects by using the SAINT[17] and SADABS[18] programs. All structures were solved by using the program library SHELXT.[19] Subsequent difference Fourier calculations and full-matrix least-squares refinement against F^2 were performed with SHELXL-2018[19] using OLEX2.[20] All non-hydrogen atoms were refined with anisotropic displacement parameters. Full details including crystal data and results of the structural refinements for each of the analyses in this report are available in the Supporting Information (Table S1).

Computational Analyses. All computational analyses were performed with the ADF2014 program[21] by using the PBEsol-D3 functional with a ZORA scalar relativistic correction and valence double-ζ+ polarization, a relativistically optimized (DZP) Slater-type basis set, with small frozen cores.[22] All computations were carried out in the gas phase at zero Kelvin, and no zero-point energy corrections were applied. See the Supporting Information for additional details.

RESULTS

The reaction of $Re_2(CO)_{10}$ with C_2H_2 in CD_2Cl_2 in the presence of Me_3NO yielded two yellow dirhenium complexes $Re_2(CO)_9(NMe_3)$ (**6**) (15% yield) and $Re_2(CO)_9[\eta^1$-*E*-2-CH=CH(NMe_3)] (**7**) (13.0 mg, 25% yield) in 15 min. The yields of **6** and **7** did not change significantly when the reaction was conducted under an atmosphere of NMe_3 (1 atm), but when the reaction of $Re_2(CO)_{10}$ with NMe_3 and Me_3NO was performed in the absence of C_2H_2, the yield of **6** increased to 40% and no **7** was obtained, as expected. Bergamo et al. provided the first evidence for the existence of **6** in their studies of the reactions of $Re_2(CO)_{10}$ with Me_3NO in THF solvent.[16] Compounds **6** and **7** were both characterized by a combination of IR, ^1H NMR, and single-crystal X-ray diffraction analyses.

An ORTEP diagram of the molecular structure of compound **6** is shown in Figure 1. Compound **6** is a simple NMe_3 derivative of $Re_2(CO)_{10}$. The NMe_3 ligand was derived from Me_3NO, which lost its O atom in the reaction with a CO ligand in $Re_2(CO)_{10}$. The NMe_3 ligand occupies an equatorial coordination site on one of the Re atoms *cis* to the Re−Re single bond in **6**. The Re−Re bond is significantly longer, 3.0938(2) Å, than the Re−Re bonds in $Re_2(CO)_{10}$, 3.041(1) Å,[23] $Re_2(CO)_9[N(H)Me_2]$, 3.0482(4) Å,[24a] and $Re_2(CO)_9(NCMe)$, 3.039(1) Å.[24b] This is certainly due in part to the presence of the sterically bulky NMe_3 ligand on Re(1), Re1−N1 = 2.334(4) Å, which is pushed away for the Re−Re bond, Re2−Re1−N1 = 101.64(9)°, by the CO ligands on the neighboring Re atom. As can be seen, the equatorial ligands on the two rhenium atoms exhibit a clear staggered relationship to one another as found in $Re_2(CO)_{10}$.[23] The ^1H NMR spectrum for **6** exhibits a singlet at δ = 3.05 for the methyl groups on the NMe_3 ligand.[16]

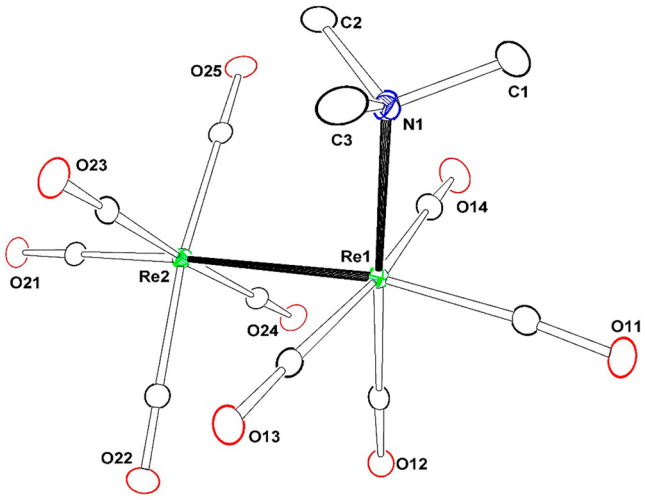

Figure 1. ORTEP diagram of the molecular structure of $Re_2(CO)_9(NMe_3)$ (**6**) showing a 20% thermal ellipsoid probability. Selected interatomic bond distances (Å) and angles (deg) are as follows: Re1−Re2 = 3.0938(2), Re1−N1 = 2.334(4), and Re2−Re1−N1 = 101.64(9).

An ORTEP diagram of the molecular structure of **7** is shown in Figure 2. There are three independent formula equivalents of **7a**−**c** in the asymmetric crystal unit of compound **7**. They are all structurally similar. Compound **7** contains a $Re_2(CO)_9$ group similar to that observed in **6**. The Re−Re bond is slightly shorter than those in **6**, Re1a−Re2a = 3.0515(3) Å, [Re1b−Re2b = 3.0578(3) Å], and [Re1c−Re2c = 3.0566(3) Å]. The most interesting ligand in **7** is a trimethylammonioethenyl ligand [η^1-*E*-2-CH=CH($^+NMe_3$)] of the type **I** (Scheme 3), which is terminally coordinated to the rhenium atom Re(1) in an equatorial coordination site by the carbon atom C1, Re1a−C1a = 2.200(4) Å, [Re1b−C1b = 2.194(5) Å], and [Re1c−C1c = 2.200(4) Å]. There is a C=C double bond to the neighboring carbon atom C2: C1a=C2a = 1.318(6) Å, C1b=C2b = 1.296(6) Å, C1c=C2c = 1.303(6) Å. The trimethylammonioethenyl ligand has *E* stereochemistry at the C=C double bond. Atom C2 is also bonded by a C−N single bond to a NMe_3 group that formally contains a positive charge on nitrogen atom N1, C2a−N1a = 1.515(6) Å, [C2b−N1b = 1.515(6) Å], and [C2c−N1c = 1.515(6) Å]. The C=C and C−N distances are similar to those observed in $[Ir(H)(C_2Ph)(-CH=CH-NEt_3)(CO)(PPh_3)_2]^+$, with C=C = 1.288(9) Å, C−N = 1.533(8) Å,[13] and in **4**, with C=C = 1.306(3) Å and C−N = 1.508(3) Å.[14] The ethenyl hydrogen atoms in **7** appear as two doublets at δ = 7.80 and 5.62 (^3J = 15

https://doi.org/10.1021/acs.inorgchem.2c01471
Inorg. Chem. 2022, 61, 12262−12274

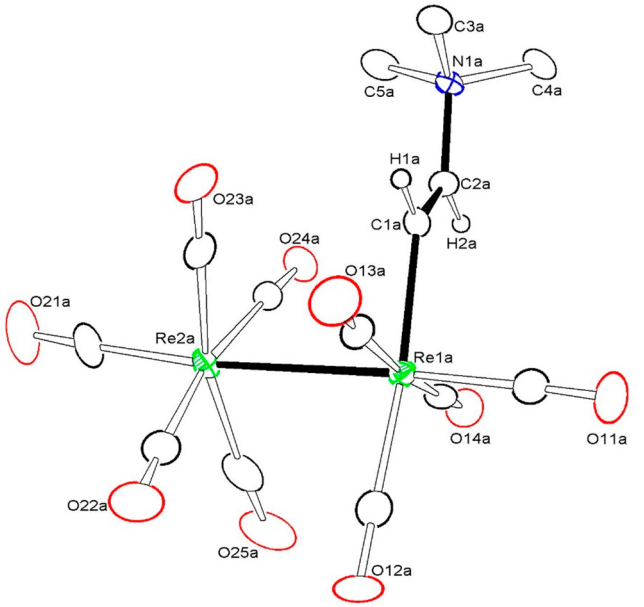

Figure 2. ORTEP diagram of the molecular structure of $Re_2(CO)_9[\eta^1$-*E*-2-CH=CH(NMe_3)] (**7**) showing a 50% thermal ellipsoid probability. Selected interatomic bond distances (Å) are as follows: molecule 1: Re1a−Re2a = 3.0515(3), Re1a−C1a = 2.200(4), C1a−C2a = 1.318(6), and C2a−N1a = 1.515(6); molecule 2: Re1b−Re2b = 3.0578(3), Re1b−C1b = 2.194(5), C1b−C2b = 1.296(6), and C2b−N1b = 1.515(6); and molecule 3: Re1c−Re2c = 3.0566(3), Re1c−C1c = 2.200(4), C1c−C2c = 1.303(6), and C2c−N1c = 1.515(6).

Hz) in the ^{1}H NMR spectrum. The resonance of the *N*-methyl groups appears at δ = 3.01. The olefinic carbon atoms C(1) and C(2) appear at δ = 134.41 and 128.34 in the ^{13}C NMR spectrum.

In further studies, it was found that compound **7** can also be obtained in reasonable yields (48%) from the reaction of **6** with C_2H_2 at 1 atm in CD_2Cl_2 solvent at 25 °C in 24 h, but this reaction is much slower than the synthesis described above (approximately 1 min). It thus seems that **6** is not an intermediate to **7** in the original reaction which provides **7** by a far more rapid route presumably involving other dirhenium species.

Compound **7** is a zwitterion. Formally, there is a positive charge on the ammonium nitrogen atom N(1a) and a negative charge on the rhenium atom Re(1a) (Figure 2). Comparisons of the infrared absorptions for the CO stretching of vibrations of compound **6** with those of **7** support this model. In particular, compound **6** is an uncharged molecule while zwitterion **7** formally contains a negative charge on Re(1). Both compounds contain similar structures for their nine terminally coordinated CO ligands and the patterns of the CO stretching absorptions in the infrared spectrum of each molecule are very similar as expected, but comparisons of the positions of the individual absorptions show that the corresponding absorptions in **7** are each approximately 10−20 cm^{-1} lower in frequency than the ones in **6**:

IR for **6**, ν_{CO}(cm^{-1} in CH_2Cl_2): 2102 (w), 2034 (s), 1986 (vs)1952 (m), 1911 (m)

IR for **7**, ν_{CO}(cm^{-1} in CH_2Cl_2): 2089 (m), 2025 (s), 1973 (vs), 1936 (s), 1894 (s)

See copies of the IR spectra in Figures S27 and S28 in the Supporting Information. The reduction in the frequencies in **7** can be explained by a weakening of CO bond strengths which would be caused by an increase in π-back bonding from the metal atoms to the π^* orbitals of the CO ligands. Reductions in CO stretching vibrational frequencies are well-established in the formation of metal carbonyl anions.[25] Our observations would be consistent with an increase in negative charge on the metal atoms as predicted by the formal charge distribution models as described above (Schemes 2 and 3) for the zwitterions reported in this study.

When the reaction of $Re_2(CO)_{10}$ with Me_3NO and C_2H_2 was performed in the presence of NEt_3, the new compound $Re_2(CO)_9(\eta^1$-*E*-2-CH=CHNEt_3) (**8**) was obtained in 20% yield together with smaller amounts of **6** (6% yield) and **7** (18% yield). Compound **8** was also characterized structurally by a single-crystal X-ray diffraction analysis. An ORTEP diagram of the molecular structure of **8** is shown in Figure 3.

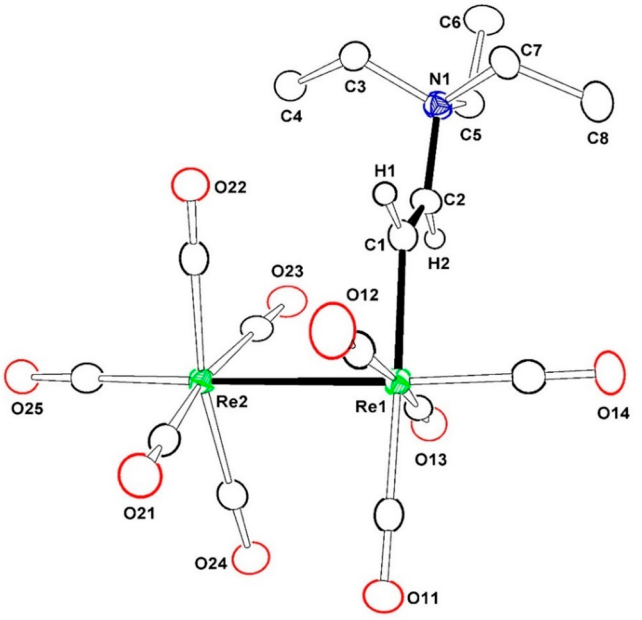

Figure 3. ORTEP diagram of the molecular structure of $Re_2(CO)_9$-$[\eta^1$-*E*-2-CH=CH(NEt_3)] (**8**), showing a 50% thermal ellipsoid probability. Selected interatomic bond distances (Å) are as follows: Re1−Re2 = 3.05569(17), Re1−C1 = 2.197(3), C1−C2 = 1.320(4), and C2−N1 = 1.530(4).

Compound **8** is structurally similar to **7** except that it contains a NEt_3 group in place of the NMe_3 group on its triethylammonioethenyl ligand on metal atom Re1, Re1−Re2 = 3.05569(17) Å and Re1−C1 = 2.197(3) Å. There is an ethenyl C=C double bond, C1=C2 = 1.320(4) Å, and C2−N1 is a single bond, C2−N1 = 1.530(4) Å. Compound **8** is also a zwitterion with a positive charge on N1 and a formal negative charge on Re(1). The ^{1}H NMR spectrum of **8** exhibits two doublets for the ethenyl protons at δ = 7.62 and 5.20 ($^3J_{H-H}$ = 16.2 Hz) and a quartet and triplet at δ = 3.10 and 1.24 ($^3J_{H-H}$ = 7.2 Hz), respectively, for the three equivalent ethyl groups.

To develop a better understanding of the bonding in these unusual zwitterionic metal complexes, molecular orbitals for a

https://doi.org/10.1021/acs.inorgchem.2c01471
Inorg. Chem. 2022, 61, 12262−12274

geometry-optimized model of compound **7** were calculated at the PBESol-D3 level. A series of selected bonding and antibonding MOs are shown in Figure 4.

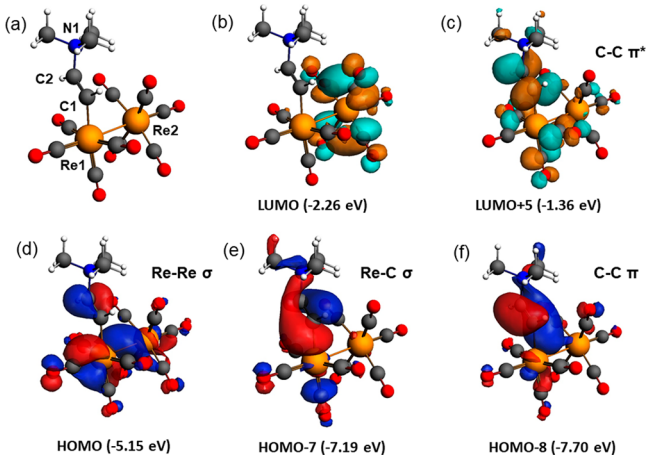

Figure 4. Selected ADF MOs for compound **7**. (a) Molecular orientation without MOs. (b) LUMO. (c) LUMO + 5. (d) HOMO. (e) HOMO − 7. (f) HOMO − 8. Energies of the MOs are given in eV.

The orientation of the molecule without orbitals is shown in Figure 4(a). The highest occupied molecular orbital (HOMO) is shown in Figure 4(d) and is composed principally of the Re−Re metal−metal bond. The MO HOMO − 7 shown in Figure 4(e) is composed principally of the σ-bond between the rhenium atom Re(1) and carbon atom C(1) of the ammonioethenyl ligand, but it also includes a component of the C−C π-bond between atoms C(1) and C(2). The C(1)−C(2) π-bond is the primary component of the HOMO − 8 shown in Figure 4(f). The large component of the antibonding version of the C(1)−C(2) π-bond is shown in the LUMO + 5 in Figure 4(c). The LUMO shown in Figure 4(b) is a combination of π^* orbitals on the equatorial CO ligands on the metal atom Re(2).

Reactions of 7 with $PMePh_2$ and PPh_3. The reaction of **7** with $PMePh_2$ in CD_2Cl_2 at 45 °C for 24 h yielded three new yellow products formulated as $Re_2(CO)_9[\eta^1$-*E*-CH═CH-$(PPh_2Me)]$ (**9a**) in 32% yield, $Re_2(CO)_9[\eta^1$-1-C(═CH_2)-$(PPh_2Me)]$ (**10a**) in 30% yield, and $Re_2(CO)_8[\mu$-η^2-C(═CH_2)$(PPh_2Me)]$ (**11a**) in 9% yield. All three products were characterized by a combination of IR, NMR, and mass spectral analyses. Compounds **10a** and **11a** were also characterized by a single-crystal X-ray diffraction analysis.

The ^{1}H NMR spectrum of **9a** showed olefinic doublets of doublets at δ = 10.12 ($^3J_{H-H}$ = 19.8 Hz, $^3J_{P-H}$ = 38.7 Hz) and 6.63 (dd, 1H, $^3J_{H-H}$ = 19.8 Hz, $^2J_{P-H}$ = 42.6 Hz). The large H−H coupling strongly indicates an *E* stereochemistry for these H atoms on a C═C double bond. The olefinic carbon atoms appeared with shifts similar to those found in **7**, δ = 122.74 ($^1J_{P-C}$ = 85 Hz), 110.03 ($^2J_{P-C}$ = 66 Hz) in the ^{13}C NMR spectrum, which suggests the presence of the η^1-*E*-2-CH═CH(PPh_2Me) ligand of the type **F** (Scheme 3) analogous to that in **7** with a PPh_2Me group in the location of the NMe_3 group. This was supported by an X-ray crystal structure determination of the related compound $Re_2(CO)_9$-$[\eta^1$-*E*-CH═CH$(PPh_3)]$ (**9b**) that was obtained from the reaction of **7** with PPh_3, *vide infra*. Compound **9a** is a zwitterion. The phosphorus atom P(1) is positively charged, and the proximate rhenium atom Re(1) formally contains a negative charge. The phosphorus resonance appears at δ = 6.55 in the ^{31}P NMR spectrum. The structure proposed for **9a** is shown in Scheme 6.

Scheme 6. Proposed Structure for 9a

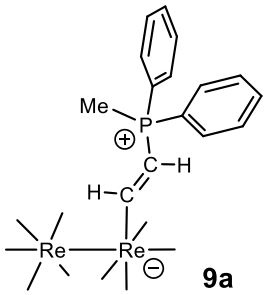

An ORTEP diagram of the molecular structure of **10a** is shown in Figure 5. Compound **10a** is structurally similar to **7**

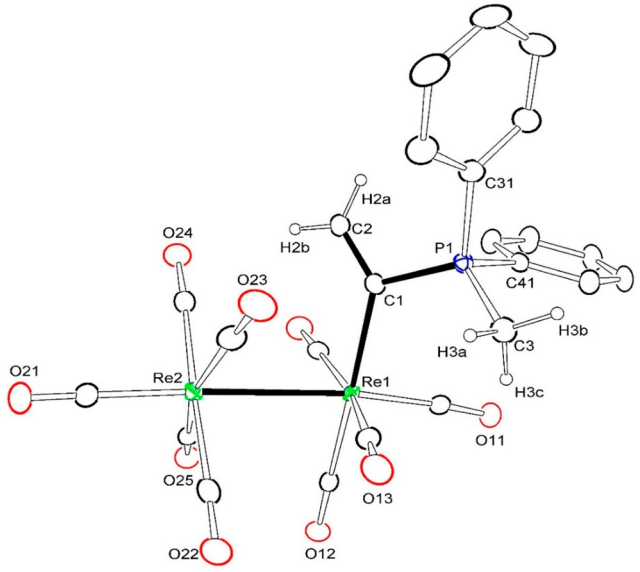

Figure 5. ORTEP diagram of the molecular structure of Re_2-$(CO)_9[\eta^1$-1-C(═CH_2)$(PPh_2Me)]$ (**10a**), showing 50% thermal ellipsoid probability. Selected interatomic bond distances (Å) are as follows: Re1−Re2 = 3.08336(16), Re1−C1 = 2.234(2), C1−C2 = 1.342(3), and C1−P1 = 1.789(3).

and **8** except that it contains a terminally coordinated 1-methyldiphenylphosphonioethenyl ligand, $[\eta^1$-1-C(═CH_2)-$(PPh_2Me)]$, of the type **G** (Scheme 3) in an equatorial coordination site on the metal atom Re(1), with Re1−C1 = 2.234(2) Å. The Re−Re single bond is long, 3.08336(16) Å, because of steric crowding, and the C1−C2 bond distance is short, 1.342(3) Å, and consistent with its formulation as a C═C double bond. There is a PPh_2Me group bonded to C(1), C1−P1 = 1.789(3) Å. Compound **10a** is a zwitterion and contains a positive charge on the phosphorus atom P(1) and a formal negative charge on the rhenium atom Re(1). There are two hydrogen atoms on carbon C(2) that appear as doublets of doublets in the ^{1}H NMR spectrum: δ = 7.09, $^3J_{P-H}$ = 74.7 Hz, $^2J_{H-H}$ = 2.1 Hz, and 6.82, $^3J_{P-H}$ = 43.2 Hz, $^2J_{H-H}$ = 2.1 Hz, with large coupling due to the phosphorus atom and very small

https://doi.org/10.1021/acs.inorgchem.2c01471
Inorg. Chem. 2022, 61, 12262−12274

coupling between the *gem*-positioned hydrogen atoms. The resonance of carbon C(2) of the phosphonioethenyl ligand was observed at δ = 154.0 in the ^{13}C NMR spectrum with no observable coupling to the phosphorus atom, while carbon C(1) was observed at δ = 123.7 with a large $^{1}J_{P-C}$ coupling of 76.9 Hz to the phosphorus atom. The phosphorus atom itself was observed at 32.90 ppm in the ^{31}P NMR spectrum. The formation of the CH_2 group implies the existence of a H−H shift in the formation of the $-C(=CH_2)(PPh_2Me)$ ligand in **10a**, *vide infra*. There have been previous reports of terminally coordinated 1-phosphonioalkenyl ligands that were prepared by the addition of phosphines to vinylidene ligands.[10a,b,11]

An ORTEP diagram of the molecular structure of **11a** is shown in Figure 6. Compound **11a** contains a 1-methyl-

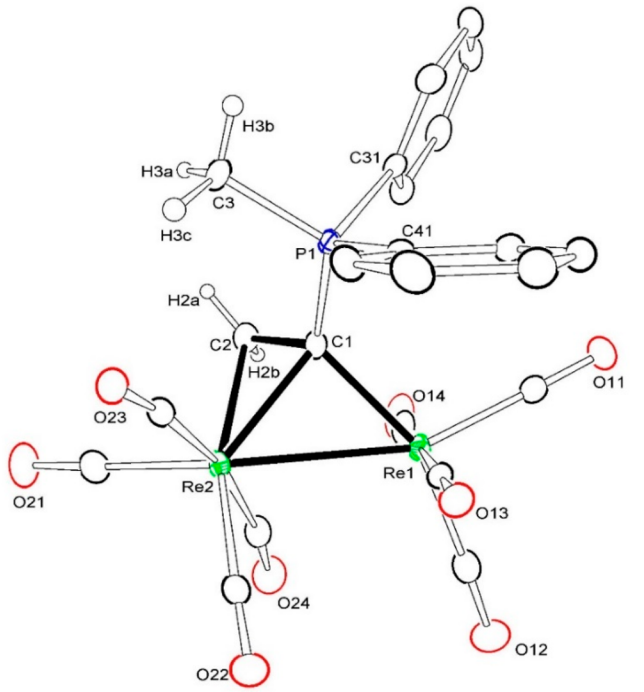

Figure 6. ORTEP diagram of the molecular structure of $Re_2(CO)_8[\mu$-η^2-1-$C(CH_2)(PPh_2Me)]$ (**11a**), showing a 40% thermal ellipsoid probability. Selected interatomic bond distances (Å) are as follows: Re1−Re2 = 2.9615(2), Re1−C1 = 2.159(3), Re2−C1 = 2.231(3), Re2−C2 = 2.275(3), C1−C2 = 1.440(4), and C1−P1 = 1.770(3).

diphenylphosphonioethenyl ligand similar to the η^1-1-C(=CH_2)(PPh_2Me) ligand in **10a** except that this phosphonioethenyl ligand bridges the two rhenium atoms in a $\sigma + \pi$ coordination by using the carbon atoms C(1) and C(2) of the C=CH_2 group. C(1) is σ-bonded to Re(1), Re1−C1 = 2.159(3) Å, and C(1) and C(2) are π-bonded to Re(2), Re2−C1 = 2.231(3) Å and Re2−C2 = 2.275(3) Å. The length of the C(1)−C(2) bond is increased to 1.440(4) Å because of its π-coordination to Re(2). This compound contains only eight CO ligands, but the Re−Re bond is still single because of the π-donation of two electrons from the C=CH_2 group to Re(2). In fact, the Re−Re bond is significantly shorter, Re1−Re2 = 2.9615(2) Å, than that in **10a** because the bridging C=CH_2 group pulls the two Re atoms together. Compound **11a** is also a zwitterion. The phosphorus atom P(1) is positively charged. The negative charge should be delocalized between the two rhenium atoms. Both metal atoms have 18-electron configurations. The two hydrogen atoms on C(2) appear as doublets of doublets at δ = 4.17 ($^{2}J_{H-H}$ = 2.5 Hz, $^{3}J_{P-H}$ = 25 Hz) and 2.46 ($^{2}J_{H-H}$ = 2.5 Hz, $^{3}J_{P-H}$ = 42 Hz) in the ^{1}H NMR spectrum because of small H−H and large P−H couplings. The phosphorus resonance appears at δ = 35.86 in the ^{31}P NMR spectrum. The coordinated carbon atoms C(1) and C(2) are shifted upfield to δ = 104.71 (C1, $^{2}J_{P-C}$ = 9 Hz) and 47.14 (C2) in the ^{13}C NMR spectrum. There have been a few previous reports of bridging 1-phosphonioalkenyl ligands.[11] Attempts to convert **9a** to **10a** or **11a** by holding a sample of **9a** dissolved in toluene-d_8 at 100 °C for 17 h were completely unsuccessful.

Compound **10a** was decarbonylated by treatment with Me_3NO in CD_2Cl_2 solvent at 48 °C for 2 h and was converted to **11a** in 55% yield by the loss of CO with the formation of one new compound $Re_2(CO)_7(\mu$-H)$[\mu$-η^3-1-$(CH_2C)P(Ph)$-$Me(o$-$C_6H_4)]$ (**12**) in 8.5% yield by the loss of two CO ligands. Conversely, when **11a** was treated with CO at 30 atm and 80 °C for 40 h, it was converted back to **10a** in 39% yield by the addition of one CO ligand (Scheme 7).

Scheme 7. Schematic of the Interconversion of Compounds 10a and 11a

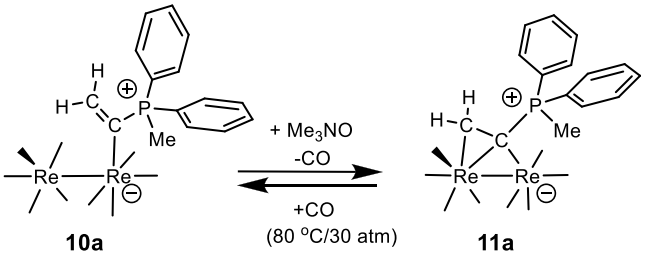

Compound **12** was also characterized by a combination of IR, NMR, and single-crystal X-ray diffraction analyses. An ORTEP diagram of the molecular structure of **12** is shown in Figure 7. Compound **12** is structurally similar to **11a** with a bridging 1-phosphonioethenyl ligand, except that one of the phenyl groups has undergone a CH activation at one of the rhenium atoms, Re(1), at an ortho position, $[\mu$-1-C(=CH_2)(P(Ph)Me)$(o$-$C_6H_4)]$, Re1−C46 = 2.231(4) Å, and there is a hydrido ligand bridging the Re−Re bond, Re1−H12 = 1.87(5) Å and Re2−H12 = 1.82(5) Å. The Re−Re bond is single, Re1−Re2 = 3.0626(2) Å, but it is much longer than the Re−Re distance in **11a** (2.9615(2) Å) because of the well-known bond-lengthening effect caused by the bridging hydrido ligand.[26] The bridging C(=CH_2) group is $\sigma + \pi$ coordinated to the two rhenium atoms: Re1−C1 = 2.263(3) Å, Re1−C2 = 2.396(4) Å, Re2−C1 = 2.200(4) Å, and C1−C2 = 1.379(5) Å. All remaining bond distances are similar to those in **11a**. The ^{1}H NMR spectrum of **12** exhibits the following prominent resonances: a singlet at δ = −13.50 for the bridging hydrido ligand and two doublets at δ = 5.56 ($^{3}J_{P-H}$ = 30.6 Hz) and 4.96 ($^{3}J_{P-H}$ = 42.6 Hz) for the *gem*-positioned hydrogen atoms on atom C(2). The phosphorus resonance was observed at δ = 41.8 in the ^{31}P NMR spectrum. Compound **12** is a zwitterion like **11a**, and both metal atoms have 18-electron configurations.

The reaction of **7** with PPh_3 in CD_2Cl_2 solvent at 48 °C for 32 h yielded two new products: $Re_2(CO)_9[\eta^1$-*E*-CH=$CH(PPh_3)]$ (**9b**) in 16% yield and $Re_2(CO)_8[\mu$-η^2-C(=$CH_2)(PPh_3)]$ (**11b**) in 32% yield. There was no evidence of a PPh_3 homologue of **10a** obtained from this reaction.

https://doi.org/10.1021/acs.inorgchem.2c01471
Inorg. Chem. 2022, 61, 12262−12274

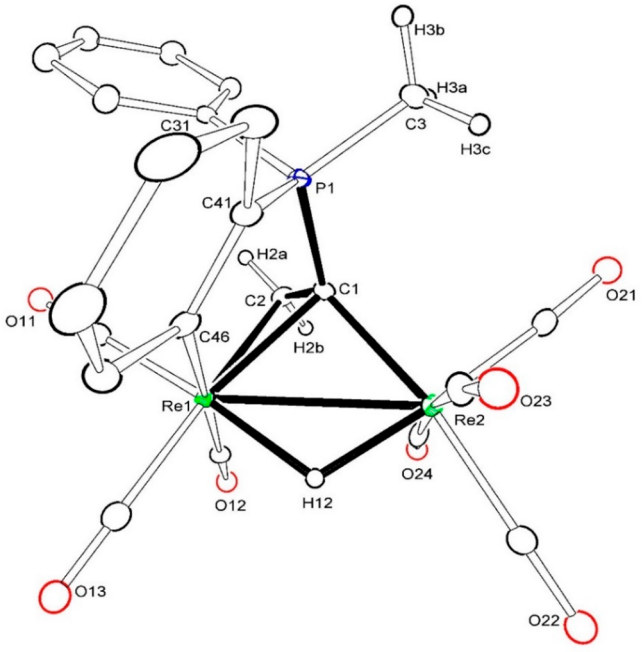

Figure 7. ORTEP diagram of the molecular structure of $Re_2(CO)_7(\mu\text{-}H)[\mu\text{-}\eta^3\text{-}1\text{-}(CH_2C)P(Ph)Me(o\text{-}C_6H_4)]$ (**12**) showing a 25% thermal ellipsoid probability. Selected interatomic bond distances (Å) are as follows: Re1−Re2 = 3.0626(2), Re1−C1 = 2.263(3), Re1−C2 = 2.396(4), Re2−C1 = 2.200(4), Re1−C46 = 2.231(4), Re1−H12 = 1.87(5), Re2−H12 = 1.82(5), C1−C2 = 1.379(5), and P1−C41 = 1.770(4).

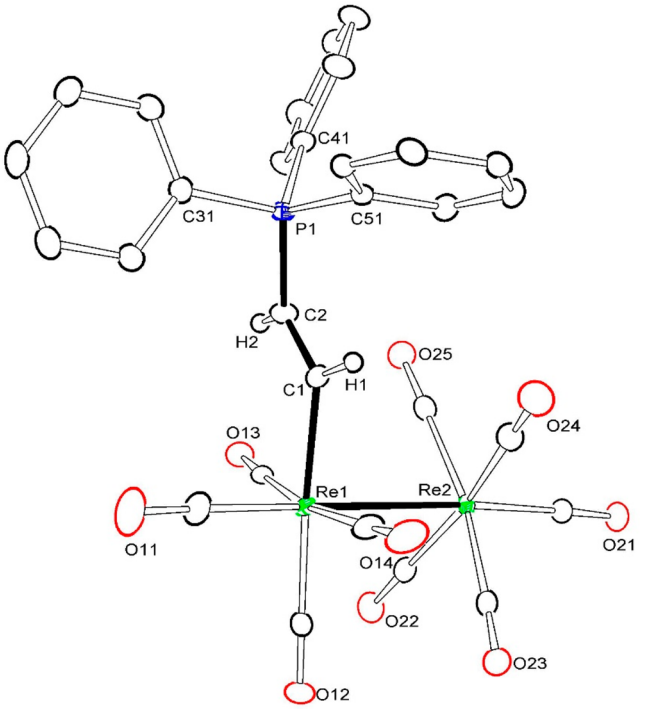

Figure 8. ORTEP diagram of the molecular structure of $Re_2(CO)_9[E\text{-}CH{=}CH(PPh_3)]$ (**9b**), showing a 40% thermal ellipsoid probability. Selected interatomic bond distances (Å) are as follows: Re1−Re2 = 3.04186(18), Re1−C1 = 2.165(3), C1−C2 = 1.341(4), and C2−P1 = 1.763(3).

Compounds **9b** and **11b** were characterized by a combination of IR, NMR, and mass spectral analyses and also by single-crystal X-ray diffraction analyses.

An ORTEP diagram of the molecular structure of **9b** is shown in Figure 8. Compound **9b** has a molecular structure similar to those of **7** and **8** and the one proposed for **9a**, see above, except that it contains a 2-triphenylphosphonioethenyl ligand, η^1-2-*E*-CH=CH(PPh_3), in the location of the ammonioethenyl ligands observed in **7** and **8**, Re1−C1 = 2.165(3) Å. The Re−Re single bond, 3.04186(18) Å, is similar in length to that observed in $Re_2(CO)_{10}$, 3.041(1) Å.[23] The C1=C2 double bond is short, 1.341(4) Å, as expected and has an *E* stereochemistry as observed in **7** and **8**. The C2−P1 single-bond length, 1.763(3) Å, is similar to the C1−P1 bond length observed in **10a** and **11a**. Compound **9b** is also a zwitterion of type **F** and similar to **7** and **8**. The phosphorus atom P(1) is positively charged, and the negative charge is formally localized on the rhenium atom Re(1). The ^{1}H NMR spectrum of **9b** exhibits two doublets of doublets at δ = 10.10 (dd, 1H, $^3J_{H-H}$ = 19.5 Hz, $^3J_{P-H}$ = 36.9 Hz) and 6.95 (dd, 1H, $^3J_{H-H}$ = 19.5 Hz, $^2J_{P-H}$ = 41.4 Hz) as a result of mutual coupling of the protons on the ethenyl carbon atoms and to the phosphorus atom on C2. The phosphorus resonance was observed at δ = 10.28 in the ^{31}P NMR spectrum.

Interestingly, we found no evidence for the formation of compounds **9b** and **11b** from an attempted reaction of $Re_2(CO)_9(PPh_3)$[27] with C_2H_2 by heating a solution in CD_2Cl_2 solvent to 45 °C for 48 h, which tends to rule out the possibility that they were formed by the insertion of C_2H_2 into the Re−P bond of $Re_2(CO)_9(PPh_3)$.

There are two independent formula equivalents of **11b** in the asymmetric crystal unit. Both molecules are structurally similar. An ORTEP diagram of the molecular structure of one of these is shown in Figure 9. Compound **11b** has virtually the same structure as **11a** except that there is a third phenyl group on the phosphorus atom of the bridging triphenylphosphonioethenyl ligand, η^2-1-C(=CH_2)(PPh_3), instead of a methyl group. Compound **11b** is also a zwitterion similar to **11a**. The two hydrogen atoms on C(2) appear as doublets of doublets at δ = 4.36 ($^2J_{H-H}$ = 2.1 Hz, $^3J_{P-H}$ = 25.2 Hz) and 2.69 ($^2J_{H-H}$ = 2.1 Hz, $^3J_{P-H}$ = 44.1 Hz) in the ^{1}H NMR spectrum with large coupling due to the phosphorus atom and small coupling between the *gem*-positioned olefinic hydrogen atoms. The phosphorus resonance appears at δ = 37.21 in the ^{31}P NMR spectrum.

It was somewhat unexpected to find the formation of zwitterions **10a**, **11a**, **11b**, and **12** which contain a C=CH_2 grouping in these reactions using the reagent HC≡CH. However, there are a number of previous reports that demonstrate the formation of vinylidene C=CH_2 ligands from ethyne, HC≡CH, by hydrogen shifts in the presence of metal atoms.[28,29] Evidence has been presented for two mechanisms for these hydrogen atom shifts: (1) a 1,2-carbon-to-carbon "concerted" hydrogen shift[28] and (2) a 1,2-hydrogen shift involving a metal-containing intermediate with a hydride and acetylide ligand formed by the oxidative addition of a CH bond to a metal atom.[29]

To gain some insight into which of these mechanisms might be preferred in the reactions with this dirhenium complex, an ADF DFT analysis of the transformation of compound **7** to **10a** was performed. This analysis began with the removal of the NMe_3 group from the structure of **7** and was followed by a geometry-optimized (GO) refinement that led to the species $Re_2(CO)_9(\eta^2\text{-}HCCH)$ (**I1**) having an η^2-coordinated C_2H_2

https://doi.org/10.1021/acs.inorgchem.2c01471
Inorg. Chem. 2022, 61, 12262−12274

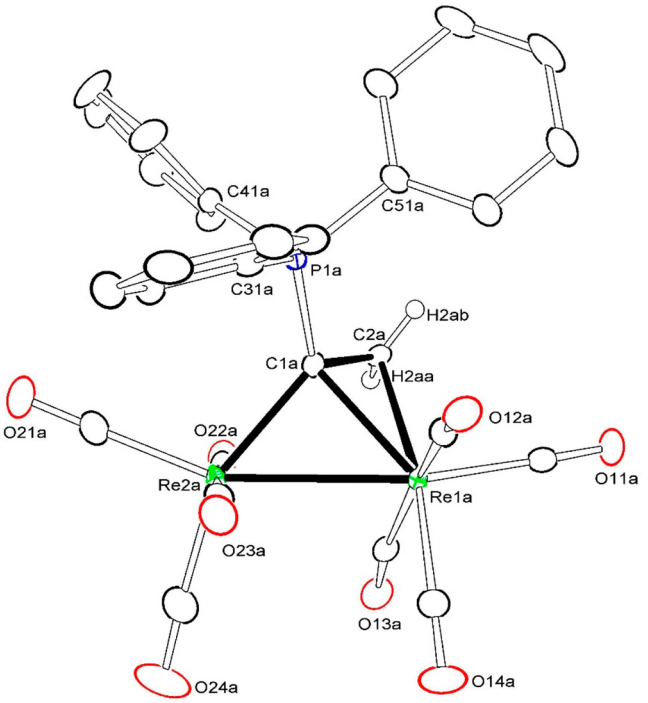

Figure 9. ORTEP diagram of the molecular structure of $Re_2(CO)_8[\mu$-η^2-$C(CH_2)PPh_3]$ (**11b**), showing a 40% thermal ellipsoid probability. Selected interatomic bond distances (Å) are as follows: Re1a−Re2a = 2.9298(2), Re1a−C1a = 2.259(3), Re1a−C2a = 2.317(3), Re2a−C1a = 2.166(3), C1a−C2a = 1.419(5), Re1b−Re2b = 2.9448(2), Re1b−C1b = 2.275(4), Re1b−C2b = 2.333(3), Re2b−C1b = 2.166(3), and C1b−C2b = 1.415(5).

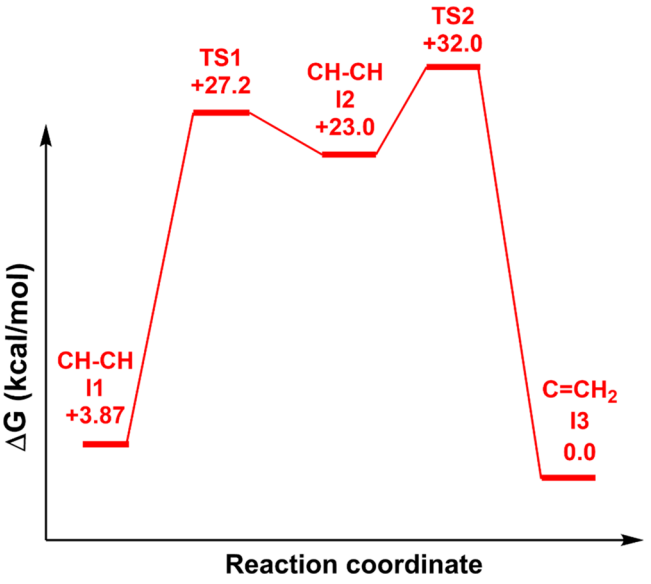

Figure 11. DFT energy-level diagram for intermediates and transition states for the transformation of a HC_2H ligand into a CCH_2 ligand in a $Re_2(CO)_9$ complex.

ligand, with C−C = 1.256 Å, in an equatorial position on one of the Re atoms. The GO structure **I1** is shown in the top left corner of Figure 10. **I1** has an energy of ΔG = +3.87 kcal relative to the final vinylidene product **I3**; see the energy-level diagram, ΔG versus the reaction coordinate, shown in Figure 11. Complex **I1** proceeded to a second intermediate **I2** via the transition state **TS1**, ΔG = +27.2 kcal/mol, having an (η^1-HCCH) ligand coordinated to one of the Re atoms by rotating the acetylene ligand around its bond to the Re atom. **TS1** proceeded spontaneously to the intermediate **I2** which contains an η^2-coordinated CH bond to the rhenium atom, with Re−C = 2.180 Å and Re−H = 1.855 Å, and the C−H bond lengthened from 1.084 Å in **I1** to 1.249 Å in **I2**. **I2** has an energy of ΔG = +23.0 kcal above the product **I3**. The next step involves a hydrogen shift to the distal carbon proceeding through the transition state **TS2**, +32.0 kcal above the product **I3**. **I3** contains a linearly coordinated η^1-C═CH_2, vinylidene ligand, terminally coordinated to only one Re atom, Re−C = 1.963 Å, and a C═CH_2 double bond of 1.305 Å. **I3** has the lowest energy across this potential energy surface.

DISCUSSION

In this work, we have obtained complexes **6** and **7** from the reaction of $Re_2(CO)_{10}$ with C_2H_2 in the presence of Me_3NO in a CD_2Cl_2 solution (Scheme 8). Compounds **6** and **7** were formed rapidly as soon as the reagents were mixed. It was subsequently found that **7** can also be obtained from **6** by reaction with C_2H_2, but this reaction is very slow (hours) at room temperature. The formation of **7** from **6** and C_2H_2 is tantamount to the insertion of a C_2H_2 molecule into the Re−N

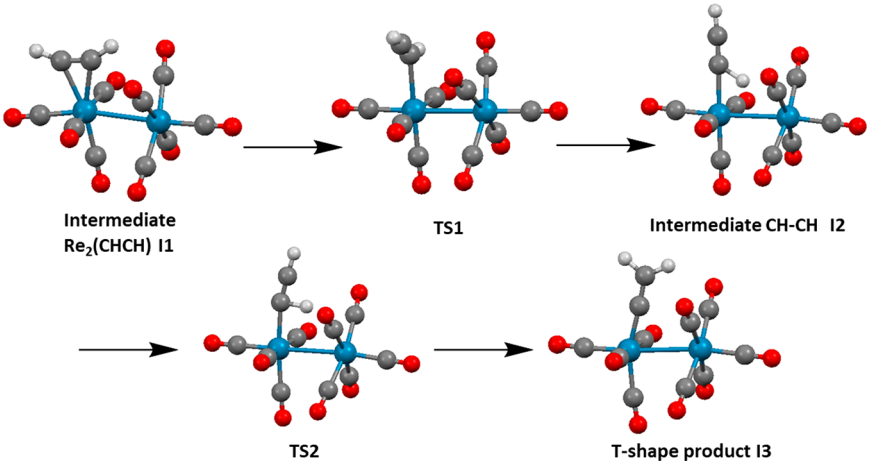

Figure 10. DFT geometry-optimized structures for the transformation of the HC_2H ligand into a CCH_2 ligand in a $Re_2(CO)_9$ complex.

https://doi.org/10.1021/acs.inorgchem.2c01471
Inorg. Chem. 2022, 61, 12262−12274

Scheme 8. Schematic of the Formation of Compounds 6−8 from $Re_2(CO)_{10}$[a]

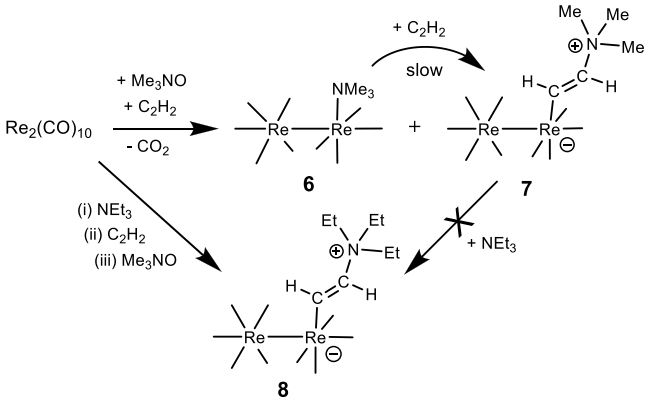

[a]+ and − signs show the assigned locations of the zwitterionic charges. The CO ligands are represented only as lines from the Re atoms.

bond of **6**. There have been reports that claim the insertion of C_2H_2 into Re−P bonds to yield phosphonioethenyl ligands,[9a,b,j] but we are skeptical of a direct insertion mechanism for the insertion of C_2H_2 into the Re−N bond of **6** because both rhenium atoms in **6** have 18-electron configurations and there is no vacant site for a precoordination of a C_2H_2 molecule. Instead, because NMe_3 is regarded as a labile ligand,[16] we favor a NMe_3/C_2H_2 substitution mechanism that would proceed through a $Re_2(CO)_9(C_2H_2)$ intermediate such as **I1** that could then re-add NMe_3 directly to one of the carbon atoms of the C_2H_2 ligand. In previous studies, we have shown that NMe_3 can be added to a C_2H_2 ligand to yield a zwitterionic ammonioethenyl ligand.[14]

In the presence of NEt_3, compounds **6** and **7** and the NEt_3 zwitterionic compound **8** were obtained from the reaction of $Re_2(CO)_{10}$ with C_2H_2 in the presence of Me_3NO (Scheme 8).

We were unable to obtain **8** from **7** by reaction with NEt_3, but **7** did react slowly with tertiary phosphines by substitution of the NMe_3 group to yield the series of zwitterionic 1- and 2-phosphonioethenyl dirhenium complexes **9a,b**, **10a**, and **11a,b** (Scheme 9). These reactions are proposed to proceed via a dissociative elimination of a molecule of NMe_3 from the ammonioethenyl ligand in **7** to yield the series of intermediates **I1**, **I2**, and **I3**, as shown in Figure 10, which proceed to yield the 2-phosphophonioethenyl compounds **9a** and **9b** by direct addition of a phosphine to a carbon atom in **I1** and the 1-phosphophonioethenyl **10a**, **11a**, and **11b** by direct addition of a phosphine to the α-vinylidene carbon atom in **I3**, respectively. The leaving-group ability of the onium group is believed to play an important role in the reactivity of onium ylides.[30]

Compounds **11a** and **12** were obtained by Me_3NO-induced decarbonylation of one and two additional CO ligands from **10a**. It is notable that **9a** cannot be transformed to **10a** or **11a**, which indicates that the H-shift on the C_2H_2 group must occur before the phosphine ligand is added to it.

CONCLUSIONS

Ethyne and selected tertiary amines, NR_3, R=Me, and Et, can be combined with a Me_3NO-decarbonylated form of $Re_2(CO)_{10}$ to yield dirhenium complexes containing terminally coordinated zwitterionic 2-trialkylammonioethenyldirhenium

Scheme 9. Schematic of the Formation of the 1- and 2-Phosphonioethenyldirhenium Carbonyl Complexes Reported in This Study from Compound 7[a]

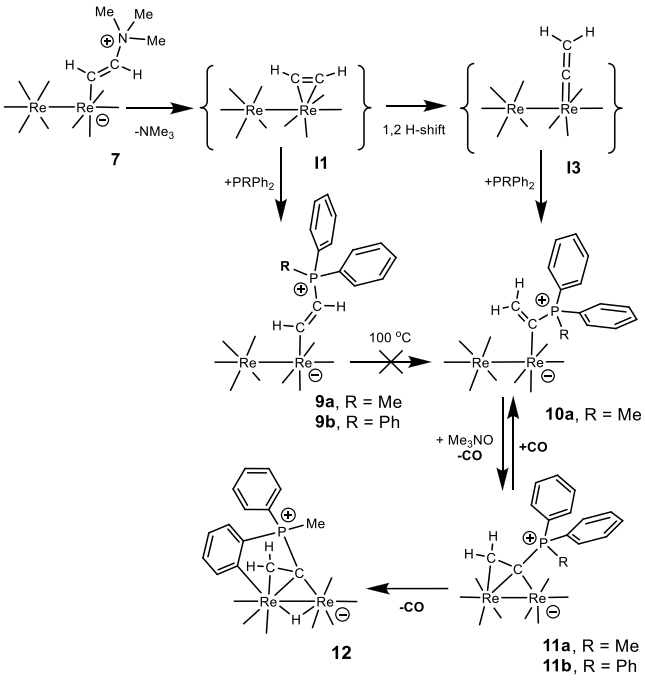

[a]+ and − signs show the assigned locations of the zwitterionic charges. The CO ligands are represented only as lines from the Re atoms.

carbonyl complexes by the formation of a C−N bond between the amine and ethyne and a Re−C bond between the second carbon atom of the ethenyl group and the rhenium atom of the $Re(CO)_4$ group. One of these complexes, **7**, was found to yield related zwitterionic 2-phosphonioethenyldirhenium complexes by the substitution of the NMe_3 group with tertiary phosphines. The reactions of **7** with tertiary phosphines also yielded zwitterionic dirhenium complexes containing terminal and (σ + π)-coordinated bridging 1-phosphonioethenyl, $H_2C{=}C(^{+}PR_3)$, ligands. DFT calculations indicate that the 1-phosphonioethenyl ligand is formed by an intramolecular 1,2-C to C hydrogen shift of an ethyne ligand to yield an incipient vinylidene, $C{=}CH_2$, ligand that is followed by the addition of a free phosphine molecule to the hydrogen-free carbon atom at the 1-position. These new zwitterionic complexes may lead to new organic molecules and ligands in reactions with selected unsaturated hydrocarbons under suitable conditions.[2,31] Further studies are in progress.

ASSOCIATED CONTENT

Supporting Information

The Supporting Information is available free of charge at https://pubs.acs.org/doi/10.1021/acs.inorgchem.2c01471.

Details of the syntheses; crystallographic analyses with structure solution and refinement details including crystallographic data and ORTEP structural diagrams; NMR spectra for new dirhenium compounds; and computational analyses with *x*, *y*, and *z* coordinates for computed structures **7**, **I1**, **TS1**, **I2**, **TS2**, and **I3** (PDF)

https://doi.org/10.1021/acs.inorgchem.2c01471
Inorg. Chem. 2022, 61, 12262−12274

Accession Codes

CCDC 2168038−2168045 contain the supplementary crystallographic data for this paper. These data can be obtained free of charge via www.ccdc.cam.ac.uk/data_request/cif, or by emailing data_request@ccdc.cam.ac.uk, or by contacting The Cambridge Crystallographic Data Centre, 12 Union Road, Cambridge CB2 1EZ, UK; fax: +44 1223 336033.

AUTHOR INFORMATION

Corresponding Author

Richard D. Adams − *Department of Chemistry and Biochemistry, University of South Carolina, Columbia, South Carolina 29208, United States;* orcid.org/0000-0003-2596-5100; Email: Adamsrd@mailbox.sc.edu

Authors

Meenal Kaushal − *Department of Chemistry and Biochemistry, University of South Carolina, Columbia, South Carolina 29208, United States*

Vitaly A. Rassolov − *Department of Chemistry and Biochemistry, University of South Carolina, Columbia, South Carolina 29208, United States;* orcid.org/0000-0002-7244-8870

Mark D. Smith − *Department of Chemistry and Biochemistry, University of South Carolina, Columbia, South Carolina 29208, United States*

Complete contact information is available at: https://pubs.acs.org/10.1021/acs.inorgchem.2c01471

Notes

The authors declare no competing financial interest.

ACKNOWLEDGMENTS

This research was supported by grant 1764192 from the National Science Foundation. The authors thank Dr. Perry Pellechia for assistance with recording the NMR spectra.

REFERENCES

(1) (a) Wittig, G.; Schollkope, U. Über Triphenyl-phosphinmethylene als olefinbildende Reagenzien I. *Chem. Ber.-Rec.* **1954**, *87*, 1318−1330. (b) Wittig, G.; Haag. Über Triphenyl-phosphinmethylene als olefinbildende Reagenzien II. *Chem. Ber.-Rec* **1955**, *88*, 1654−1666. (c) Bart, J. C. J. Structure of the Non-stabilized Phosphonium Ylid Methylenetriphenylphosphorane. *J. Chem. Soc. B* **1969**, 350−365.

(2) (a) Gessner, V. H., Ed. *Modern Ylide Chemistry: Applications in Ligand Design, Organic and Catalytic Transformations*; Structure and Bonding; Springer Pub.: Cham, Switzerland, 2018; Vol. *177*. (b) Kolodiazhnyi, O. I. *Phosphorus Ylides: Chemistry and Applications in Organic Synthesis*; Wiley-VCH: Weinheim, Germany, 1999. (c) Fan, Y. C.; Kwon, O. Advances in nucleophilic phosphine catalysis of alkenes, allenes, alkynes, and MBHADs. *Chem. Commun.* **2013**, *49*, 11588−11619. (d) Khong, S.; Venkatesh, T.; Kwon, O. Nucleophilic Phosphine Catalysis: The Untold Story. *Asian J. Org. Chem.* **2021**, *10*, 2699−2708. (e) Scharf, L. T.; Gessner, V. H. Metalated Ylides: A New Class of Strong Donor Ligands with Unique Electronic Properties. *Inorg. Chem.* **2017**, *56*, 8599−8607. (f) Guo, H.; Fan, Y. C.; Sun, Z.; Wu, Y.; Kwon, O. Phosphine Organocatalysis. *Chem. Rev.* **2018**, *118*, 10049−10293.

(3) (a) Sun, X.-L.; Tang, Y. Ylide-Initiated Michael Addition − Cyclization Reactions beyond Cyclopropanes. *Acc. Chem. Res.* **2008**, *41*, 937−948. (b) Aggarwal, V. K.; Winn, C. L. Catalytic, Asymmetric Sulfur Ylide-Mediated Epoxidation of Carbonyl Compounds: Scope, Selectivity, and Applications in Synthesis. *Acc. Chem. Res.* **2004**, *37*, 611−620. (c) Trost, B. M.; Melvin, L. S. *Sulfur Ylides: Emerging Synthetic Intermediates*; Academic Press: New York, 1975. (d) Neuhaus, J. D.; Oost, R.; Merad, J.; Maulide, N. Sulfur-Based Ylides in Transition-Metal-Catalysed Processes. In *Surfur Chemistry*; Jiang, X., Ed.; Topics in Current Chemistry; Springer: Cham, 2018; Vol. *376*, pp 429−475. (e) Lu, L.-Q.; Li, T.-R.; Wang, Q.; Xiao, W.-J. Beyond Sulfide-Centric Catalysis: Recent Advances in the Catalytic Cyclization Reactions of Sulfur Ylides. *Chem. Soc. Rev.* **2017**, *46*, 4135−4149. (f) Zhang, Y.; Wang, J. Catalytic [2,3]-Sigmatropic Rearrangement of Sulfur Ylide Derived from Metal Carbene. *Coord. Chem. Rev.* **2010**, *254*, 941−953. (g) Burtoloso, A. C. B.; Dias, R. M. P.; Leonarczyk, I. A. Sulfoxonium and Sulfonium Ylides as Diazocarbonyl Equivalents in Metal-Catalyzed Insertion Reactions. *Eur. J. Org. Chem.* **2013**, *2013*, 5005−5016. (h) Li, A.-H.; Dai, L.-X.; Aggarwal, V. K. Asymmetric Ylide Reactions: Epoxidation, Cyclopropanation, Aziridination, Olefination, and Rearrangement. *Chem. Rev.* **1997**, *97*, 2341−2372. (i) Cuenca, A. B.; Fernandez, E. Boron-Wittig olefination with gem-bis(boryl)alkanes. *Chem. Soc. Rev.* **2021**, *50*, 72−86.

(4) (a) Maryanoff, B. E.; Reitz, A. B. The Wittig Olefination Reaction and Modifications Involving Phosphoryl-Stabilized Carbanions. Stereochemistry, Mechanism, and Selected Synthetic Aspects. *Chem. Rev.* **1989**, *89*, 863−927. (b) Johnson, A. W.; Kaska, W. C.; Starzewski, K. A. O.; Dixon, D. *Ylides and Imines of Phosphorus*; Wiley: New York, 1993.

(5) (a) Sweeney, J. B. Sigmatropic rearrangements of 'onium' ylids. *Chem. Soc. Rev.* **2009**, *38*, 1027−1038. (b) Dequina, H. J.; Schomaker, J. M. Aziridinium Ylides: Underused Intermediates for Complex Amine Synthesis. *Trends Chem.* **2020**, *2*, 874−887. (c) Jiang, K.; Chen, Y.-C. Organocatalytic reactions involving nitrogen-ylides. *Tetrahedron Lett.* **2014**, *55*, 2049−2055. (d) Roiser, L.; Zielke, K.; Waser, M. Ammonium Ylide Mediated Cyclization Reactions. *Asian J. Org. Chem.* **2018**, *7*, 852−864. (e) Funt, L. D.; Novikov, M. S.; Khlebnikov, A. F. New applications of pyridinium ylides toward heterocyclic synthesis. *Tetrahedron* **2020**, *76*, 131415. (f) Nicastri, K. A.; Zappia, S. A.; Pratt, J. C.; Duncan, J. M.; Ilia, A.; Guzei, I. A.; Fernández, I.; Schomaker, J. M. Tunable Aziridinium Ylide Reactivity: Noncovalent Interactions Enable Divergent Product Outcomes. *ACS Catal.* **2022**, *12*, 1572−1580. (g) Vanecko, J. A.; Wan, J.; West, F. G. Recent advances in the Stevens rearrangement of ammonium ylides. Application to the synthesis of alkaloid natural products. *Tetrahedron* **2006**, *62*, 1043−1062. (h) Clark, J. S. In *Nitrogen, Oxygen and Sulfur Ylide Chemistry: A Practical Approach in Chemistry*; Clark, J. S., Ed.; Oxford University Press: New York, 2002; Chapter 1. (i) Ranjith, J.; Ha, H.-J. Synthetic Applications of Aziridinium Ions. *Molecules* **2021**, *26*, 1774. (j) Lahm, G.; Pacheco, J. O. C.; Opatz, T. Rearangements of Nitrile-Stabilized Ammonium Ylides. *Synthesis* **2014**, *46*, 2413−2421.

(6) (a) Lapointe, S.; Sarbajna, A.; Gessner, V. H. Ylide-Substituted Phosphines: A Platform of Strong Donor Ligands for Gold Catalysis and Palladium-Catalyzed Coupling Reactions. *Acc. Chem. Res.* **2022**, *55*, 770−782. (b) Scherpf, T.; Schwarz, C.; Scharf, L. T.; Zur, J.-A.; Helbig, A.; Gessner, V. H. Ylide-functionalized phosphines: Strong Donor Ligands for Homogeneous Catalysis. *Angew. Chem., Int. Ed.* **2018**, *57*, 12859. (c) Wang, J. In *Comprehensive Organometallic Chemistry III*; Mingos, D. M. P., Crabtree, R. H., Eds.; Elsevier: Oxford, 2007; Vol. *11*; pp 151−178.

(7) Selected examples include (a) Pattacini, R.; Jiez, S.; Braunstein, P. Facile dichloromethane activation and phosphine methylation. Isolation of unprecedented zwitterionic organozinc and organocobalt Intermediates. *Chem. Commun.* **2009**, 890−892. (b) Engelter, C.; Moss, J. R.; Niven, M. L.; Nassimbeni, L. R.; Reid, G. A cationic ylide complex of platinum (II): its structure and formation from a chloromethyl-platinum complex. *J. Organomet. Chem.* **1982**, *232*, C78−C80. (c) Kermode, N. J.; Lappert, M. F.; Skelton, B. W.; White, A. H.; Holton, J. Synthesis of ylideplatinum(II) complexes via α-functionalised alkylplatinum(II) intermediates and some comparative data on palladium(II) complexes; X-ray structure of trans-[Pt-$(CH_2PEt_3)I(PEt_3)_2$]I. *J. Organomet. Chem.* **1982**, *228*, C71−C75. (d) Azam, K. A.; Frew, A. A.; Lloyd, B. R.; Manojlovic-Muir, L.; Muir, K. W.; Puddephatt, R. J. (μ-Methylene)diplatinum complexes: their

syntheses, structures, and properties. *Organometallics* **1985**, *4*, 1400−1406. (e) Churchill, M. R.; Wasserman, H. J. Crystal and molecular structure of $[W(CH_2PMe_3)(CO)_2Cl(PMe_3)_3][CF_3SO_3]$, a seven-coordinate tungsten(II) complex produced by transfer of a trimethylphosphine to the W:CH_2 system. *Inorg. Chem.* **1982**, *21*, 3913−3916. (f) Toupet, L.; Weinberger, B.; Abbayes, H. D.; Gross, U. Structure du Complexe Tetracarbonyle-(methylenetriphenylphosphorane-C)fer(II), $[Fe(C_{19}H_{17}P)(CO)_4]$. *Acta Crystallogr. Sect. C: Cryst. Struct. Commun.* **1984**, *40*, 2056−2058. (g) Moss, J. R.; Niven, M. L.; Stretch, P. M. Haloalkyl complexes of the transition metals. Part 5. The synthesis and reactions of some new pentamethylcyclopentadienyl halomethyl and methoxymethyl complexes of molybdenum (II) and tungsten (II) and the X-ray crystal structure of the cationic ylide complex $[\eta$-$C_5Me_5W(CO)_3CH_2PPh_3]$ I. *Inorg. Chim. Acta* **1986**, *119*, 177−186. (h) Porter, L. C.; Knachel, H.; Fackler, J. P., Jr. A Mononuelear Gold(l) Complex Containing a Covalently Bound Ylide Ligand. The Structure of Chloro[methyl(methylene)diphenylphosphoranyI-C] gold (I). *Acta Crystallogr.* **1987**, *C43*, 1833−1835. (i) Uson, R.; Laguna, A.; Uson, A.; Jones, P. G.; Meyer-Base, K. Synthesis of Pentafluorophenyl-(ylide)silver(l) Complexes: X-Ray Structures of two Modifications of $[Ag(C_6F_5)(CH_2PPh_3)]$. *J. Chem. Soc., Dalton Trans.* **1988**, 341−345. (j) Uson, R.; Laguna, A.; Laguna; Gimeno, M. C.; de Pablo, A.; Jones, P. G.; Meyer-Base, K.; Erdbrugger, C. F. Synthesis and reactivity of neutral complexes of the types $[AuX_3(ylide)]$ and trans-$[Au(C_6F_5)X_2(ylide)]$ (X = halide or pseudohalide). X-ray structure of $[Au(SCN)_3(CH_2PPh_3)]$. *J. Organomet. Chem.* **1987**, *336*, 461−468. (k) Hoover, J. F.; Stryker, J. M. Synthesis of Platinum Bis-(phosphonium ylide) Complexes from -Halomethyl Precursors. *Organometallics* **1988**, *7*, 2082−2084. (l) Cerrada, E.; Concepcion Gimeno, M.; Laguna, A.; Laguna, M.; Orera, V.; Jones, P. G. Charge-transfer salts with mononuclear and dinuclear ylide gold(I) complexes: X-ray structure of $[Au(CH_2PPh_3)_2](TCNQ)$, (TCNQ = 7,7′,8,8′-tetracyanoquinodimethane). *J. Organomet. Chem.* **1996**, *506*, 203−210.

(8) Selected examples include (a) O'Connor, E. J.; Helquist, P. Stable precursors of transition-metal carbene complexes. Simplified preparation and crystal structure of (η^5-cyclopentadienyl)-[(dimethylsulfonium)methyl]dicarbonyliron(II) fluorosulfonate. *J. Am. Chem. Soc.* **1982**, *104*, 1869−1874. (b) Hevia, E.; Perez, J.; Riera, V.; Miguel, D. Manganese(I) and Rhenium(I) Tricarbonyl-(Alkylthio)methyl and Alkylidenesulfonium Complexes. *Organometallics* **2002**, *21*, 5312−5319. (c) Leoni, P.; Marchetti, F.; Paoletti, M. Synthesis of Palladium Sulfonium Ylides and the Structures of *trans*-$[PdCl(CH_2SR_2)(PBu^t{}_2H)_2]X$ (X=CF_3SO_3, SR_2) Tetrahydrothiophene; X= PF_6, R = Et). *Organometallics* **1997**, *16*, 2146−2151. (d) Kilbourn, B. T.; Felix, D. The Crystal Structure of Methyldineopentylsulphonium Tri-iododineopentylsulphonium-methylzincate, $[(C_5H_{11})_2SMe]^+[(C_5H_{11})_2SCH_2ZnI_3]^-$. *J. Chem. Soc. A* **1969**, 163−168. (e) Fackler, J. P., Jr.; Paparizos, C. Trimethylgold(III) Complexes of Reactive Sulfoxonium and Sulfonium Ylides. *J. Am. Chem. Soc.* **1977**, *99*, 2363−2364. (f) Vicente, J.; Chicote, M.-T.; Abrisqueta, M. D.; Alvarez-Falcon, M. M.; de Arellano, M. C. R.; Jones, P. G. New Carbenegold(I) Complexes Synthesized by the "Acac Method. *Organometallics* **2003**, *22*, 4327−4333.

(9) (a) Lappas, D.; Hoffman, D. M.; Folting, K.; Huffman, J. C. Synthesis and Structure of a Resonance Stabilized (Trimethylphosphonio)metallapropenide. *Angew. Chem., Int. Ed. Engl.* **1988**, *27*, 587−589. (b) Hoffman, D. M.; Huffman, J. C.; Lappas, D.; Wierda, D. A. Alkyne Reactions with Rhenium(V) Oxo Alkyl Phosphine Complexes—Phosphine Displacement versus Apparent Re-P Insertion. *Organometallics* **1993**, *12*, 4312−4320. (c) Rogers, R. D.; Alt, H. G.; Maisel, H. E. Die Molekülstruktur des carbenartigen Ylidkomplexes $(C_5H_4Me)(CO)_2Mn[CHCH(PEt_3)]$. *J. Organomet. Chem.* **1990**, *381*, 233−238. (d) Chin, C. S.; Lee, S.; Oh, M.; Won, G.; Kim, M.; Park, Y. J. *cis*-Bis(alkenyl)iridium(III) Compounds by Apparent Insertion of Two Acetylenes into Two Ir-P Bonds: Crystal Structures of *cis, trans*-$[IrCl(-CH{=}CH^+PPh_3)_2(CO)(PPh_3)_2]^{2+}$ and $[Ir(OClO_3)(CH_3)(H_2O)(CO)(PPh_3)_2]^+$. *Organometallics* **2000**, *19*, 1572−1577. (e) Chin, C. S.; Park, Y.; Kim, J.; Byeongno Lee, B. Facile Insertion of Alkynes into Ir-P (Phosphine) and Ir-As (Arsine) Bonds: Second and Third Alkyne Addition to Mononuclear Iridium Complexes. *J. Chem. Soc., Chem. Commun.* **1995**, 1495−1496. (f) Takats, J.; Washington, J.; Santarsiero, B. D. Condensation of $Os(CO)_4(\eta^2$-HCCH) with $CpRh(CO)(PR_3)$. Unexpected Phosphine Dependence in the Formation of Dimetallacycles: Reverse Regiochemistry and a Zwitterionic Compound. *Organometallics* **1994**, *13*, 1078−1080. (g) Yang, K.; Bott, S. G.; Richmond, M. G. Regioselective phosphine attack on the coordinated alkyne in $Co_2(\mu$-alkyne) complexes Reactivity studies and X-ray diffraction structures of $Co_2(CO)_4$(bma)-(μ-HC≡C^{t}Bu) and the zwitterionic hydrocarbyl complexes $Co_2(CO)_4[(\mu$-η^2:η^2:η^1:η^1:-RC=C(R′)PPh_2C=C(PPh_2)C(O)C-(O)]. *J. Organomet. Chem.* **1996**, *516*, 65−80. (h) Bott, S. G.; Shen, H.; Senter, R. A.; Richmond, M. G. Acetylide Participation in Ligand Substitution and P-C Bond Cleavage in the Reaction between $HRu_3(CO)_9([(\mu_3$-η^2:η^2:η^1-C≡CPh) and 4,5-Bis-(diphenylphosphino)-4-cyclopenten-1,3-dione (bpcd). Syntheses and X-ray Structures of $HRu_3(CO)_7[[(\mu_3$-η^2:η^2:η^1:η^1:η^1-$Ph_2PC{=}CC(O)CH_2C(O)PPh_2C{=}CPh]$ and $Ru_3(CO)_7((\mu$-η^2:η^1:-PhC=CHPh)[(μ-η^2:η^1:-PPhC=CC(O)CH_2C(O)PPh_2]. *Organometallics* **2003**, *22*, 1953−1959. (i) Allen, A., Jr.; Lin, W. Unprecedented Insertion of Alkynes into a Palladium-Phosphine Bond. A Facile Route to Palladium-Bound Alkenyl Phosphorus Ylides. *Organometallics* **1999**, *18*, 2922−2925. (j) Shih, K.-Y.; Tylicki, R. M.; Wu, W.; Fanwick, P. E.; Walton, R. A. Reactions of monodentate tertiary phosphines with the dirhenium(II) alkyne complexes $[Re_2Cl_3(\mu$-dppm)$_2$(CO)(η^2-RCCH)]X (X=PF_6 or O_3SCF_3) to form ylides. *Inorg. Chim. Acta* **1995**, *229*, 105−112.

(10) (a) Boland-Lussier, B. F.; Churchill, M. R.; Hughes, R. P.; Rheingold, A. L. Synthesis and characterization of cationic iron vinylidene compounds: formation of carbon-hydrogen, carbon-nitrogen and carbon-phosphorus bonds and the x-ray crystal structure of $[Fe(\eta$-$C_5H_5)(CO)(PPh_3)\{C(PPh_3){=}CH_2\}]^+BF_4^-$. *Organometallics* **1982**, *1*, 628−634. (b) Krivykh, V. V.; Valyaev, D. A.; Utegenov, K. I.; Mazhuga, A. M.; Taits, E. S.; Semeikin, O. V.; Petrovskii, P. V.; Godovikov, I. A.; Glukhov, I. V.; Ustynyuk, N. A. Protonation of Zwitterionic Manganese and Rhenium Phosphoniostyryl Complexes (η^5-C_5H_5)$(CO)_2$M-C(+PR_3)=C(H)Ph: Experimental and DFT Study. *Eur. J. Inorg. Chem.* **2011**, *2011*, 201−211. (c) Ipaktschi, J.; Munz; Thomas Klotzbach, T. Phosphorus-Substituted η^1-Vinylidene Tungsten Complexes: Synthesis and Cyclization. *Organometallics* **2005**, *24*, 206−213. (d) Kolobova, N. E.; Skripkin, V. V.; Aleksandrov, G. G.; Struchkov, Y. T. Synthesis of cationic iron complexes with the cyclobutenylidene ligand. The crystalline structure of 1-triphenylphosphonium-2-phenylvinyl-η^5-cyclopentadienyldicarbonylirontetrafluoroborate. *J. Organomet. Chem.* **1979**, *169*, 293−300.

(11) (a) Hogarth, G.; Knox, S. A. R.; Lloyd, B. R.; Macpherson, K. A.; Morton, D. A. V.; Orpen, A. G. Structural Observation of Bis(diphenylphosphino)methane Reactivity at a Di-iron Centre: Crystal Structures of Isomeric $[Fe_2(CO)_5(\mu$-CHCHCO){μ-P(Ph_2)-CH_2PPh_2}], $[Fe_2(CO)_6(\mu$-C(CH_2)P(Ph_2)CH_2PPh_2}] and $[Fe_2(CO)_2\{\mu$-C(CH_2Ph)P(Ph_2)CH_2PPh}]. *J. Chem. Soc., Chem. Commun.* **1988**, 360−362. (b) Bamber, M.; Froom, S. F. T.; Green, M.; Schulz, M.; Werner, H. Nucleophilic attack by isocyanides, phosphines and cyclohexenesulphide on the α-carbon of "side-on" bonded μ-σ:η^2-(4e)-vinylidenes; formation of thioketene and thioaldehyde dimolybdenum complexes. *J. Organomet. Chem.* **1992**, *434*, C19−C25.

(12) Henrick, K.; McPartlin, M.; Deeming, A. J.; Hasso, S.; Manning, P. Addition of dimethylphenylphosphine to μ- and μ_3-alkynyl and μ_3-allenyl ligands in triosmium clusters: X-ray crystal structures of three zwitterionic adducts. *J. Chem. Soc., Chem. Commun.* **1982**, 899−906.

(13) (a) Chin, C. S.; Lee, H.; Oh, M. Reactions of Iridium(III) Compounds with Alkynes in the Presence of Triethylamine: The First Example of M-CH=CH-$^+NR_3$. *Organometallics* **1997**, *16*, 816−818. (b) Chin, C. S.; Cho, H.; Won, G.; Oh, M. Reaction of an

https://doi.org/10.1021/acs.inorgchem.2c01471
Inorg. Chem. 2022, 61, 12262−12274

(Alkyl)(alkenyl)(alkynyl)iridium(III) Complex with HCl: Intramolecular C-C Bond Formation from Alkyl, Alkenyl, and Alkynyl Groups Coordinated to "$Ir(CO)(PPh_3)_2$". H/D Exchange between CH_3 and DCl. *Organometallics* **1999**, *18*, 4810−4816.
(14) Adams, R. D.; Smith, M. D.; Wakdikar, N. D. Zwitterionic Ammoniumalkenyl Ligands in Metal Cluster Complexes. Synthesis, Structures and Transformations of Zwitterionic Trimethylammoniumalkenyl Ligands in Hexaruthenium Carbido Carbonyl Complexes. *Inorg. Chem.* **2020**, *59*, 1513−1521.
(15) Adams, R. D.; Akter, H.; Kaushal, M.; Smith, M. D.; Tedder, J. D. Synthesis, Structures, and Transformations of Bridging and Terminally - Coordinated Trimethylammonioalkenyl Ligands in Zwitterionic Pentaruthenium Carbido Carbonyl Complexes. *Inorg. Chem.* **2021**, *60*, 3781−3793.
(16) Bergamo, M.; Beringhelli, T.; D'Alfonso, G.; Mercandelli, P.; Moret, M.; Sironi, A. Hydrido-Carbonyl Chain Clusters. Synthesis, Solid State Structure, and Solution Behavior of the Tetranuclear Open Cluster Anions $[Re_4H(\mu\text{-}H)_2(CO)_{17}]^-$ and $[Re_4(\mu\text{-}H)(CO)_{18}]^-$. *Organometallics* **1997**, *16*, 4129−4137.
(17) *APEX3*, version 2016.5-0 and *SAINT*, version 8.37A; Bruker AXS, Inc.: Madison, WI.
(18) SADABS Version 2016/2. Krause, L.; Herbst-Irmer, R.; Sheldrick, G. M.; Stalke, D. *J. Appl. Crystallogr.* **2015**, *48*, 3−10.
(19) SHELXT: Sheldrick, G. M. SHELXT - Integrated space-group and crystal-structure determination. *Acta Crystallogr.* **2015**, *A71*, 3−8.
(20) **OLEX2**: a complete structure solution, refinement and analysis program. Dolomanov, O. V.; Bourhis, L. J.; Gildea, R. J.; Howard, J. A. K.; Puschmann, H. *J. Appl. Crystallogr.* **2009**, *42*, 339−341.
(21) (a) te Velde, G.; Bickelhaupt, F. M.; van Gisbergen, S. J. A.; Fonseca Guerra, C.; Baerends, E. J.; Snijders, J. G.; Ziegler, T. Chemistry with ADF. *J. Comput. Chem.* **2001**, *22*, 931−967. (b) ADF2014, SCM, *Theoretical Chemistry*; Vrije Universiteit: Amsterdam, The Netherlands, http://www.scm.com.
(22) (a) Fonseca Guerra, C.; Snijders, J. G.; te Velde, G.; Baerends, E. J. Towards an order-N DFT method. *Theor. Chem. Acc.* **1998**, *99*, 391−403. (b) Perdew, J. P.; Ruzsinszky, A.; Csonka, G. I.; Vydrov, O. A.; Scuseria, G. E.; Constantin, L. A.; Zhou, X.; Burke, K. Restoring the density-gradient expansion for exchange in solids and surfaces. *Phys. Rev. Lett.* **2008**, *100*, 136406. (c) Perdew, J. P.; Ruzsinszky, A.; Csonka, G. I.; Vydrov, O. A.; Scuseria, G. E.; Constantin, L. A.; Zhou, X.; Burke, K. Restoring the Density-Gradient Expansion for Exchange in Solids and Surfaces. *Phys. Rev. Lett.* **2009**, *102*, 039902. (d) van Lenthe, E.; Baerends, E. J.; Snijders, J. G. Relativistic regular two-component Hamiltonians. *J. Chem. Phys.* **1993**, *99*, 4597−4610. (e) van Lenthe, E.; Baerends, E. J.; Snijders, J. G. Relativistic total energy using regular approximations. *J. Chem. Phys.* **1994**, *101*, 9783−9792. (f) van Lenthe, E.; Ehlers, A. E.; Baerends, E. J. Geometry optimizations in the zero-order regular approximation for relativistic effects. *J. Chem. Phys.* **1999**, *110*, 8943−8953.
(23) Churchill, M. R.; Amoh, K. N.; Wasserman, H. J. Redetermination of the crystal structure of dimanganese decacarbonyl and determination of the crystal structure of dirhenium decacarbonyl. Revised values for the Mn-Mn and Re-Re bond lengths in $Mn_2(CO)_{10}$ and $Re_2(CO)_{10}$. *Inorg. Chem.* **1981**, *20*, 1609−1611.
(24) (a) Adams, R. D.; Dhull, P. Formyl C-H activation in N,N-Dimethylformamide by a dirhenium carbonyl complex. *J. Organomet. Chem.* **2017**, *849*−*850*, 228−232. (b) Adams, R. D.; Chen, L.; Wu, W. Reactions of Alkynes Having Electron-Withdrawing Substituents with $Re_2(CO)_9(NCMe)$. Formation of Trans Dimetalated Olefins by Alkyne Insertion into an Re-Re Bond. *Organometallics* **1993**, *12*, 1257−1265.
(25) Zhou, M.; Andrews, L.; Bauschlicher, C. W., Jr. Spectroscopic and Theoretical Investigations of Vibrational Frequencies in Binary Unsaturated Transition-Metal Carbonyl Cations, Neutrals, and Anions. *Chem. Rev.* **2001**, *101*, 1931−1961.
(26) Bau, R.; Drabnis, M. H. Structures of transition metal hydrides determined by neutron diffraction. *Inorg. Chim. Acta* **1997**, *259*, 27−50. (b) Teller, R. G.; Bau, R. Crystallographic Studies of Transition-Metal Hydride Complexes. *Structure and Bonding*; Springer: Berlin, 1981; Vol. *41*, pp 1−82.
(27) Koelle, U. Aminoxidinduzierte Ligandensubstitution an Ubergandsmetallcarbonylen. II. *J. Organomet. Chem.* **1978**, *155*, 53−62.
(28) (a) Wakatsuki, Y.; Koga, N.; Werner, H.; Morokuma, K. An ab Initio MO Study on the Transformation of Acetylene to Vinylidene in the Coordination Sphere of Rhodium(I). The Intra- and Intermolecular Proton Transfer Mechanism. *J. Am. Chem. Soc.* **1997**, *119*, 360−366. (b) Wakatsuki, Y.; Koga, N.; Yamazaki, H.; Morokuma, K. Acetylene π-Coordination, Slippage to σ-Coordination, and 1,2-Hydrogen Migration Taking Place on a Transition Metal. The Case of a Ru(II) Complex As Studied by Experiment and ab Initio Molecular Orbital Simulations. *J. Am. Chem. Soc.* **1994**, *116*, 8105−8111.
(29) (a) Cowley, M. J.; Lynam, J. M.; Slattery, J. M. A mechanistic study into the interconversion of rhodium alkyne, alkynyl hydride and vinylidene complexes. *Dalton Trans.* **2008**, 4552−4554. (b) Xiao, J.; Cowie, M. Alkyne-to-Vinylidene Tautomerism Mediated by Two Adjacent Metal Centers. Structures of $[Ir_2I_2(CO)_2(\mu\text{-}CC(H)R)(Ph_2PCH_2PP_2)_2]$ (R = H, Ph). *Organometallics* **1993**, *12*, 463−472. (c) Silvestre, J.; Hoffmann, R. Hydrogen Migration in Transition Metal Alkyne and Related Complexes. *Helv. Chim. Acta* **1985**, *68*, 1461−1506. (d) Cabeza, J. A.; Pérez-Carreño, E. P. The Bridging Acetylene to Bridging Vinylidene Rearrangement in a Triruthenium Carbonyl Cluster: A DFT Mechanistic Study. *Organometallics* **2010**, *29*, 3973−3978.
(30) Aggarwal, V. K.; Harvey, J. N.; Robiette, R. On the Importance of Leaving Group Ability in Reactions of Ammonium, Oxonium, Phosphonium, and Sulfonium Ylides. *Angew. Chem., Int. Ed.* **2005**, *44*, 5468−5471.
(31) Xie, C.; Smaligo, A. J.; Song, X.-R.; Kwon, O. Phosphorus-Based Catalysis. *ACS Cent. Sci.* **2021**, *7*, 536−558.

https://doi.org/10.1021/acs.inorgchem.2c01471
Inorg. Chem. 2022, 61, 12262−12274